AD NUMBER

ADB014070

LIMITATION CHANGES

TO:

Approved for public release; distribution is unlimited.

FROM:

Distribution authorized to U.S. Gov't. agencies only; Test and Evaluation; SEP 1976. Other requests shall be referred to Air Force Weapons Laboratory, DYT, Kirtland AFB, NM 87117.

AUTHORITY

AFWL LTR, 29 APR 1985

AD B014070

AUTHORITY: AFWL ltr, 29 Apr 85

AFWL-TR-76-183

AFWL-TR-
76-183

(2)

THE HULL HYDRODYNAMICS COMPUTER CODE

September 1976

Mark A. Fry, Capt, USAF
Richard E. Durrett, Major, USAF
Gary P. Ganong, Major, USAF
Daniel A. Matuska, Major, USAF
Mitchell D. Stucker, Capt, USAF
Burton S. Chambers
Charles E. Needham
Cydnes D. Westmoreland

Final Report

AIR FORCE WEAPONS LABORATORY
Air Force Systems Command
Kirtland Air Force Base, NM 87117

AFWL-TR-76-183

This final report was prepared by the Air Force Weapons Laboratory, Kirtland Air Force Base, New Mexico, under Job Order 88091816. Captain Mitchell D. Stucker (DYT) was the Laboratory Project Officer-in-Charge.

When US Government drawings, specifications, or other data are used for any purpose other than a definitely related Government procurement operation, the Government thereby incurs no responsibility nor any obligation whatsoever, and the fact that the Government may have formulated, furnished, or in any way supplied the said drawings, specifications, or other data is not to be regarded by implication or otherwise as in any manner licensing the holder or any other person or corporation or conveying any rights or permission to manufacture, use, or sell any patented invention that may in any way be related thereto.

This technical report has been reviewed and is approved for publication.

Mitchell D. Stucker

MITCHELL D. STUCKER
Captain, USAF
Project Officer

FOR THE COMMANDER

Donald B. Mitchell

DONALD B. MITCHELL
Lt Colonel, USAF
Chief, Theoretical Branch

John S. DeWitt

JOHN S. DEWITT
Lt Colonel, USAF
Chief, Technology Division

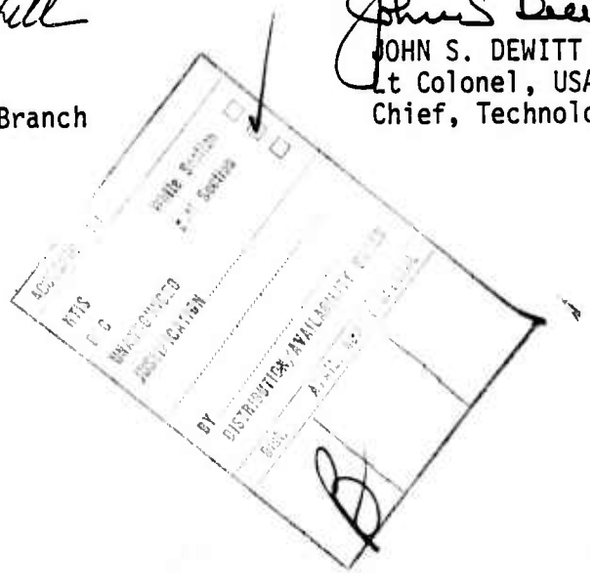

DO NOT RETURN THIS COPY. RETAIN OR DESTROY.

UNCLASSIFIED

SECURITY CLASSIFICATION OF THIS PAGE (When Date Entered)

REPORT DOCUMENTATION PAGE

READ INSTRUCTIONS BEFORE COMPLETING FORM

(14) REPORT NUMBER: AFWL-TR-76-183

2. GOVT ACCESSION NO.

3. RECIPIENT'S CATALOG NUMBER

4. TITLE (and Subtitle): (6) THE HULL HYDRODYNAMICS COMPUTER CODE.

5. TYPE OF REPORT & PERIOD COVERED: (9) Final Report

6. PERFORMING ORG. REPORT NUMBER

7. AUTHOR(s): (10) Mark A. Fry, Capt, USAF; Richard E. Durrett, Maj, USAF; Gary P. Ganong, Maj, USAF; Daniel A. Matuska, Maj, USAF; Mitchell Stucker, Capt, USAF (See Block 18)

8. CONTRACT OR GRANT NUMBER(s)

9. PERFORMING ORGANIZATION NAME AND ADDRESS

Air Force Weapons Laboratory (DYT)
Kirtland Air Force Base, NM 87117

10. PROGRAM ELEMENT, PROJECT, TASK AREA & WORK UNIT NUMBERS

62601F
88091816

11. CONTROLLING OFFICE NAME AND ADDRESS

Air Force Weapons Laboratory (DYT)
Kirtland Air Force Base, NM 87117

(11) 12. REPORT DATE: Sep 1976 — (12) 48p.

13. NUMBER OF PAGES: 50

14. MONITORING AGENCY NAME & ADDRESS (if different from Controlling Office): (16) AF-8809

15. SECURITY CLASS. (of this report): UNCLASSIFIED

15a. DECLASSIFICATION/DOWNGRADING SCHEDULE

16. DISTRIBUTION STATEMENT (of this Report)

Distribution limited to US Government agencies only because test and evaluation information concerning military systems is discussed in the report (Sep 1976). Other requests for this document must be referred to AFWL (DYT), Kirtland AFB, NM 87117.

17. DISTRIBUTION STATEMENT (of the abstract entered in Block 20, if different from Report)

(17) 880918

18. SUPPLEMENTARY NOTES

Additional authors are: Burton S. Chambers
Charles E. Needham
Cydney D. Westmoreland

19. KEY WORDS (Continue on reverse side if necessary and identify by block number)

Hydrodynamics code
Second order differencing
Preprocessor dynamic dimensions and higher language fortran
Two and three dimension Eulerian

20. ABSTRACT (Continue on reverse side if necessary and identify by block number)

The HULL (Hydrodynamics Unlimited) code is a family of hydrocodes at the Air Force Weapons Laboratory. Within the code are contained two and three-dimensional Eulerian difference schemes which are first and second order accurate. Many computational aids such as different types of automatic rezone and library update of problem information exist within the code. HULL has been used to study fireball rise phenomenology, free field air blast, interaction of air blast with rigid structures, nozzle problems, shallow buried

→ next page (over)

DD FORM 1 JAN 73 1473 EDITION OF 1 NOV 65 IS OBSOLETE

UNCLASSIFIED

SECURITY CLASSIFICATION OF THIS PAGE (When Date Entered)

013150

ABSTRACT (continued)

cont. munitions, high altitude phenomenology, as well as others. The code is dynamic and modular and allows one to quickly adapt it to a particular problem.

SUMMARY

The following sections describe in report form for the first time the HULL code. Since the code itself is quite large and required the work of dozens of people to produce the capability that the code now offers, one cannot expect to learn all the pertinent details from this report. However, one can begin to appreciate the power that the code provides as a scientific tool. The basic HULL code is a hydrodynamics code that numerically solves the equations of mass, momentum and energy conservation.

How these equations are solved and how the results compare to experimental evidence will be examined.

PREFACE

This report was prepared from contributions of many individuals and is meant to serve as an introduction to the HULL computer code. The development of the HULL code involved a large number of people and involved many man-years of effort. We would like to express our thanks to the following people who have contributed many hours of hard work to this effort: Reginald Clemens of Science Applications Inc , Lewis Gaby, John Prentice and Mike Tower all from the Air Force Weapons Laboratory.

CONTENTS

ILLUSTRATIONS

SECTION I

INTRODUCTION

This report describes the HULL code, which is used at the Air Force Weapons Laboratory (AFWL) to theoretically investigate hydrodynamic phenomena of interest to the Air Force. Usual problems of interest involve atmospheric response (e.g., air blast, heave, etc.) to large-scale rapid energy deposition (e.g., nuclear and high explosive detonations).

The HULL code (or simply HULL) is actually a system of computer codes used primarily for hydrodynamic calculations, and hence is normally referred to as a hydrocode. Where possible, its operation is automatic to allow the user time to run and analyze calculations instead of doing burdensome bookkeeping. The system is written in a higher-level language, which when compiled generates Control Data Corporation (CDC) extended FORTRAN and a few somewhat system-oriented routines written in assembly language. Utilizing the higher-level language allows one to produce a large variety of codes by specifying certain options at the beginning of a run.

The HULL code, initiated in September 1971, had evolved through 88 separate versions by June 1976. It continues to be modified in order to allow the addition of new options as well as improvements in numerical techniques. The current version consists of approximately 44000 lines of code and can be obtained from the AFWL for users with legitimate needs for the code.

Basically, HULL is a multidimensional (two or three) Eulerian hydrodynamics code. For two-dimensional problems, Cartesian or cylindrical geometry is available, whereas for three-dimensional problems only Cartesian geometry is available at present. Two finite difference schemes may be used--the SHELL version, and the more recent HULL version which treats the flow second order accurate in a Lagrangian phase and then fluxes mass, momentum and energy to maintain the original spatial grid. The latter method is the one described in the sequel. Additional options available include seven different rezone techniques, three equations of state, single or multi-materials (any number), variable zone size, three atmospheres, massless trace particles or massive noninteractive and/or interactive particles (e.g., dust), water vapor, rigid bodies within the mesh, equilibrium radiation diffusion, a strength formulation, magnetohydrodynamics

formulation, and an option for handling a nuclear air blast precursor. The magnetohydrodynamics formulation has recently been made operational and the strength formulation is still being checked out.

The HULL code is based upon numerical techniques and algorithms that have been developed by many individuals and organizations over a period of many years.

Historically, the development of large Eulerian hydrocodes began with Harlow's SHELL-PIC code at Los Alamos in 1955 (ref. 1). SHELL-PIC used the particle-in-cell method for the numerical solution of the hydrodynamic equations. Due to its Eulerian nature, SHELL-PIC was able to effect a solution to the hydrodynamic equations even when large distortions were present in the fluid.

To provide a good theoretical picture of the phenomenology of atmospheric detonations, the AFWL acquired two versions of SHELL, developed at General Atomic by Freeman, Johnson and others for hypervelocity impact studies. The first version, SHELL-PIC, was based on Harlow's code. The second code, SHELL-OIL, was a continuum version (ref. 2). Comparison of PIC and OIL calculations of late time phenomenology of the BLUEGILL Event (ref. 3) demonstrated the superiority of the continuous, SHELL-OIL method over the discrete, particle-in-cell method for that class of problem.

In 1965, at the request of Defense Atomic Support Agency, the AFWL modified SHELL-OIL (hereafter called SHELL) to allow the calculation of high-explosive detonation phenomena (ref. 4). The first event calculated was DISTANT PLAIN (refs. 5 and 6). The AFWL then added a multi-material capability to SHELL to allow preshot computation of DISTANT PLAIN Event 6 (ref. 7). Since then, the AFWL has continued to provide numerical calculations in support of Defense Nuclear Agency's high explosive tests (refs. 8 through 12).

In addition to the high explosive computations, the AFWL performed over 40 calculations of various yields and heights of burst during the period 1965 to 1970 in support of systems vulnerability and ionization threat analyses (refs. 13 and 14). During this same period, SHELL was modified to study dust and pebble clouds (refs. 15, 16 and 17). The incorporation of variable zone size permitted the study of nuclear air blast precursors (refs. 18 and 19). The addition of fine material capability and radiation diffusion enabled us to study nuclear weapon detonation phenomena (refs. 20 and 21).

Since 1970, other versions of SHELL were written in spherical (ref. 22) and Cartesian (ref. 23) coordinates. SHELL was also rewritten to run on the ILLIAC IV computer (ref. 24).

By 1971 many versions of SHELL existed (more than 20 separate decks) making modifications to the code difficult. This situation, when coupled with the desire to improve the finite difference scheme in SHELL, led Durrett and Matuska of AFWL to develop the HULL system. In order to contain in one system a great multiplicity of versions, it was decided to write HULL in a higher ordered language. This language required a compiler, which was written by Captain Lewis Gaby of AFWL and was given the name SAIL. The output of SAIL is primarily FORTRAN, although some assembly code does exist. With the higher ordered language, Durrett and Matuska were able to structure HULL so that (1) modifications to the various versions of the code could be made easily, (2) typical calculations were run three times as fast, and (3) restrictions on the number of zones or number of materials, etc., disappeared (i.e., a problem's size becomes limited only by the computer's capabilities in terms of central memory, disc space, etc., instead of DIMENSION statements).

Since 1971 additional modifications have been made in the HULL system by other contributors such as Clemens of SAI (advanced plotting and system capabilities), Fry of AFWL (magnetohydrodynamics), Tower of AFWL (strength formulation), Gaby of AFWL (radiation diffusion), Chambers of AFWL (nuclear air blast precursors), Needham of AFWL (advances in burn routines and equations of state), Prentice of AFWL (auxiliary debugging aids), and Westmoreland of AFWL (extensive revisions to KEEL and one-dimensional versions of HULL).

By June 1976, HULL was on version 88 and development continues for various types of problems as the need arises. Currently a library of almost 300 problems exists.

It is worthwhile to note that the development for HULL has primarily been based on the study of fireball growth and rise phenomena, and the prediction of free field air blast as well as the effect of rigid structures on the air blast. For these applications, HULL has been shown to perform very well when utilized in the fashion that was intended.

The remainder of this report discusses the architecture and operating philosophy, the differential equations and the difference technique, and experimental and theoretical comparisons.

SECTION II

ARCHITECTURE AND OPERATING PHILOSOPHY

This section briefly describes the architecture and operating philosophy of HULL. The motivation for developing HULL was to provide (1) flexibility in making revisions either to improve or add options, (2) speed while executing and (3) removal of restrictions on size that are dictated by the inadequacies of pure FORTRAN. In order to accomplish these goals it was necessary to write HULL in a language of higher level than FORTRAN; this is referred to as the Executive Language.

It was also necessary to write a compiler for the Executive Language, which was named SAIL. The combination of Executive Language, FORTRAN, and assembly language that comprises the HULL system is a SAIL input file. It consists of a set of card-images which the user can modify if and when appropriate. With the flexibility obtained with the higher-level language it was possible to automate many burden tasks, but at the expense of many man-years of code development closely tied to the operating system being utilized. With this generality available in the HULL system, auxiliary programs were developed to perform some specialized functions, many of which were designed to automate as much as practical the use of HULL on a day to day basis. These include programs BOW, PLANK and STERN.

BOW creates and maintains a library tape (or LIBTAPE) which contains information on the status of various jobs or problems running under the HULL system. Each problem run by HULL is assigned a unique problem number for identification. BOW basically keeps a current record of the data tapes for each problem, and has a list of unused tapes which are assigned to the various problems as necessary. STERN is executed at the end of each HULL run and updates the library tape with information on the tapes used during the run.

PLANK builds the HULL code for each run using as input cards read from the input deck, information from the HULL data tape, and the card image information on the launch file.

To gain insight into how these are utilized, the following example shows how a typical run might proceed.

The INPUT file is read into the computer. It consists of control cards and other input, generally in the form of a card deck. Execution of this run begins by fetching the HULL code from the disc. Then, user-generated changes are made to the codes that are specified in the INPUT file, and the remainder of the INPUT file is copied to TAPE5. The library tape is then assigned to the job and BOW executes. The BOW code reads the problem numbers and other start parameters from TAPE5. It then reads the library tape, finds the appropriate problem record, and selects the correct HULL data tape to restart the calculation. BOW then asks the operator to mount the HULL data tape, which contains all the hydrodynamic variables, by reference to its location in the computer tape library. When this tape is mounted, BOW terminates.

PLANK executes next. It reads the problem number and other start information from TAPE5. It then reads the HULL data tape and selects the appropriate cycle for restart. Having found the correct cycle, PLANK reads certain information off the tape and with this information decides which HULL code to generate. PLANK is, in addition to other things, a compiler which reads the Executive Language from the card images on the SAIL file and creates from them a complete FORTRAN code which it puts on an appropriate file. At this point PLANK terminates. The FTN compiler is then invoked and compiles the FORTRAN code. The compiled version of HULL is then loaded and executed, and will run until a stop condition is sensed. This is typically 4 to 5 hours or until problem completion.

STERN executes after HULL terminates. STERN requests that the library tape be mounted and then updates the problem information record to reflect the changes made in problem status on this run.

There also exists in the HULL system great amounts of code that make it possible to safely allow operators to terminate calculations, and then to later restart these calculations at the point where they were previously terminated, without any user intervention. The operator only need resubmit the same deck. This automatic restart feature has evolved at the AFWL during the last two decades. This feature makes life somewhat more tolerable during periods of frequent system crashes, power outages and other abnormal means of program termination.

The data tapes that are written and contain the data necessary to restart serve as a large data bank for future analysis. Since each of these calculations take tens of hours on a CDC 6600, it is desirable to save the data.

SECTION III

DIFFERENTIAL EQUATIONS AND DIFFERENCE TECHNIQUES

This section presents the differential equations being solved with HULL and the difference techniques utilized. This report considers only the hydrodynamic calculation. Other reports will address the magnetohydrodynamics, radiation diffusion, and the strength formulations.

1. THE HULL 2D DIFFERENCE METHOD

The difference method employed by the HULL code is a fully second order accurate method developed by Matuska. The equations below describe a compressible, nonconducting and inviscid fluid.

Conservation of Mass

$$\frac{d\rho}{dt} + \rho(\nabla \cdot \vec{u}) = 0 \tag{1}$$

Conservation of Momentum

$$\rho \frac{d\vec{u}}{dt} + \nabla p = - \rho \vec{g} \tag{2}$$

Conservation of Energy

$$\rho \frac{dE}{dt} + \nabla \cdot (p\vec{u}) = - \rho \vec{u} \cdot \vec{g} \tag{3}$$

Equation of State

$$p = f(\rho, I) \tag{4}$$

where

ρ = material density (gm/cm^3)

P = pressure (dynes/cm^2)

$\vec{u}$ = (u,v) fluid velocity (cm/sec)

$E = I + \frac{\vec{u} \cdot \vec{u}}{2}$ (ergs/gm)

I = internal specific energy (ergs/gm)

$\vec{g}$ = gravitational acceleration (cm/gm^2)

t = time (sec)

The procedure is to solve the first four equations in two phases. In phase I, we solve the equations within a Lagrangian framework. Equations (2) and (3) are treated in this phase. The second phase treats equation (1) in a manner which causes dissipation of kinetic energy into internal energy, especially in regions of large velocity gradients.

$$\frac{d\rho}{dt} + \rho\left(\frac{1}{R}\frac{\partial(Ru)}{\partial R} + \frac{\partial V}{\partial z}\right) = 0 \tag{5}$$

$$\rho\frac{dU}{dt} + \frac{\partial P}{\partial R} = 0 \tag{6}$$

$$\rho\frac{dV}{dt} + \frac{\partial P}{\partial z} = -\rho g \tag{7}$$

$$\rho\frac{dE}{dt} + \frac{1}{R}\frac{\partial(RPU)}{\partial R} + \frac{\partial}{\partial Z}(PV) = -\rho V g \tag{8}$$

where

R = radial coordinate

Z = axial coordinate

U = component of $\vec{u}$ in the radial direction

V = component of $\vec{u}$ in the axial direction

In establishing finite difference analogs to equations 5 through 8 we consider a discrete subset of F(R,Z,T) by defining

$$F(I,J,N) = F(R(I),Z(J),T(N))$$

where R(I), Z(J), and T(N) are particular values of R, Z, and T, respectively, and the I, J, and N assume integer values in the range 1 to IMAX for I, 1 to JMAX for J, and 0 to NMAX for N. The R(I) and I(J) are defined in terms of a given set of DR(I) and DZ(J) such that

R(I) = R(0) + (SUM, K=1, I-1, (DR(K))) + DR(I)/2 for I=2,...,IMAX
R(1) = R(0) + DR(1)/2
R(J) = Z(0) + (SUM,K=1,J-1,(DZ(K)))+DZ(J)/2 for J-2,...,JMAX
Z(1) = Z(0) + DZ(1)/2

where R(0) and Z(0) have some specified values.

The hydrodynamic variables ρ, U, V, and I (internal specific energy) are defined for each set of coordinates (I,J) at a particular time T(N). The pressure P(I,J,N) is defined at each point by the equation of state (equation 4).

Interpolated values for the hydrodynamic variables of the form F(I+1/2,J,N), F(I,J+1/2,N), or F(I,J,N+1/2), or similar forms, are defined in terms of the F(I,J,N). In general,

$$F(I+1/2,J,N) = (F(I+1,J,N) + F(I,J,N))/2$$

and

$$F(I,J+1/2,N) = (F(I,J+1,N) + F(I,J,N))/2.$$

This definition will apply except where explicitly noted.

a. Phase I

In method 2 the finite difference analogs to equations (6) through (8) are chosen as

$$U(I,J,N+1) = U(I,J,N)-DT*(P(I+1/2,J,N+1/2)-P(I-1/2,J,N+1/2))/(\rho(I,J,N)*DR(I)) \quad (9)$$

$$V(I,J,N+1) = V(I,J,N)-DT*(P(I,J+1/2,N+1/2)-P(I,J-1/2,J,N+1/2))/(\rho(I,J,N)*DZ(J))-DT*G(J) \quad (10)$$

$$E(I,J,N+1) = E(I,J,N)-DT/\rho(I,J,N)*((R(I+1/2)*P(I+1/2,J,N+1/2)*U(I+1/2,J,N+1/2)-R(I-1/2)*P(I-1/2,J,N+1/2)*U(I-1/2,J,N+1/2))/(R(I)*DR(I))+(P(I,J+1/2,N+1/2)*V(I,J+1/2,N+1/2)-P(I,J-1/2,N+1/2)*V(I,J-1/2,N+1/2))/DZ(J)/-DT*V(I,J,N+1)*G(J) \quad (11)$$

where

DT = T(N+1)-T(N)

R(I+1/2) = R(I)+DR(I)/2

R(I-1/2) = R(I)-DR(I)/2

Z(J+1/2) = Z(J)+DZ(J)/2

Z(J-1/2) = Z(J)-DZ(J)/2

G(J) = VALUE OF G AT Z(J).

All the values appearing in equations (9) through (11) are immediately known except the time advanced (N+1/2) values for pressure and velocity. These time advanced values are used so that the approximations to the partial derivatives appearing in equations (6) through (8) may be centered in time and space. In the case where

$$DR(I) = \text{constant} \qquad \text{For } I=1,\ldots,IMAX$$

and

$$DZ(J) = \text{constant} \qquad \text{For } J=1,\ldots,JMAX,$$

this produces a fully second order accurate difference method. In a region where the DR(I) and DZ(J) are not constant the second order accuracy is lost. This adversely affects the stability of the first phase calculation. The amount of instability which may be obtained is related to the magnitude of the incremental changes in DR(I) and DZ(J).

Most of the computations in the first phase are expended in obtaining the time advanced values for pressure and velocity. The time advanced velocities are obtained by differencing equations (6) and (7) as

$$U(I+1/2,J,N+1/2) = U(I+1/2,J,N)-DT/(2*\rho(I+1/2,J,N+1/2)) *((P(I+1,J,N)-P(I,J,N))/(R(I+1)-R(I))) \qquad (12)$$

$$V(I,J+1/2,N+1/2) = V(I,J+1/2,N)-DT/(2*\rho(I,J+1/2,N+1/2)) *((P(I,J+1,N)-P(I,J,N))/(Z(J+1)-Z(J))) -G(J+1/2)*DT/2 \qquad (13)$$

where

$$G(J+1/2) = (G(J)+G(J+1))/2.$$

The time advanced densities appearing in equations (12) and (13) are obtained by differencing equation (5) as

$$\rho(I+1/2,J,N+1/2) = \rho(I+1/2,J,N)*(1-DT/(2*R(I+1/2))*(R(I+1)*U(I+1,J,N)-R(I)*U(I,J,N))/(R(I+1)-R(I))) \quad (14)$$

$$\rho(I,J+1/2,N+1/2) = \rho(I,J+1/2,N)*(1-DT/2*(V(I,J+1,N)-V(I,J,N))/(Z(J+1)-Z(J))) \quad (15)$$

where

$$\rho(I+1/2,J,N) = M(I,J,N)+M(I+L,J,N))/(\pi*(R(I+3/2)**2-R(I+1/2)**2)*DZ(J))$$

$$\rho(I,J+1/2,N) = (M(I,J,N)+M(I,J+1,N))/\pi*(R(I+1/2)**2-R(I-1/2)**2)*(DZ(J)+DZ(J+1)))$$

and the mass associated with a point (I,J,N) is defined by

$$M(I,J,N) = \rho(I,J,N)*(\pi*(R(I+1/2)**2-R(I-1/2)**2)*DZ(J))$$

where $\pi = 3.14159...$ and $R(I+3/2) = R(I+1) + DR(I+1)/2.$

The time advanced pressure appearing in equations (9) through (11) requires a little more effort. First, an alternative energy equation can be obtained from equations (2) and (3) as

$$\rho \frac{dI}{dt} + P\vec{\nabla} \cdot \vec{u} = 0 \quad (16)$$

An effective γ can be defined by

$$\gamma = 1 + \frac{P}{\rho I} \quad (17)$$

We will assume for the purposes of calculating a half time step advanced pressure, which in turn is used in approximating the partial derivatives in equations (9) through (11), that the Lagrangian derivative with respect to time of

γ is small and can be ignored. In application, it is only required that the change in γ at a particular point be small over a time of DT/2.

Taking the Lagrangian derivative with respect to time in equation (17) and using equations (1) and (16), we can write

$$\frac{dP}{dt} + \gamma P\vec{\nabla} \cdot \vec{u} = 0 \tag{18}$$

Equation (18) is used to obtain time advanced pressures given by

```
P(I+1/2,J,N+1/2) = P(I+1/2,J,N)*(1-DT*γ(I+1/2,J,N)*(R(I+1)
                   *U(I+1,J,N)-R(I)*U(I,J,N))/(2*R(I+1/2)*(R(I+1)
                   -R(I))))

P(I,J+1/2,N+1/2) = P(I,J+1/2,N)*(1-DT*γ(I,J+1/2,N)
                     *(V(I,J+1,N)-V(I,J,N))/(2*(Z(J+1)-Z(J))))
```

where γ is defined from equation (17) as

$$\gamma(I+1/2,J,N) = 1+P(I+1/2,J,N)/(\rho(I+1/2,J,N)*I(I+1/2,J,N))$$

$$\gamma(I,J+1/2,N) = 1+P(I,J+1/2,N)/(\rho(I,J+1/2,N)*I(I,J+1/2,N)).$$

All quantities needed to solve equations (9), (10), and (11) are now defined. Solution of these equations will complete a second order accurate Lagrangian calculation. The next step would normally be that of transporting mesh vertices. Instead we choose to flux the hydrodynamic quantities to retain the original mesh configuration. This calculation is done in phase II.

b. Phase II

Changes in density are computed in phase II by calculating a mass flux between mesh points and then transporting the appropriate amount of mass from point to point. The transported mass carries with it a proportionate amount of internal energy and momentum. The velocities and specific internal energy are then redefined at each mesh point by conserving momentum and total energy at that point.

The mass flux between mesh points is defined as the product of the interpolated velocity, the density as defined by solution of equation (1), the intermediate cross sectional area, and the time step. The equations are:

$$MF(I+1/2,J,N+1) = U(I+1/2,J,N+1)*\rho(I+1/2,J,N+1)*2*\pi*R(I+1/2)*DZ(J)*DT$$

$$MF(I,J+1/2,N+1) = V(I,J+1/2,N+1)*\rho(I,J+1/2,N+1)*2*\pi*R(I)*DR(I)*DT$$

where the time advanced densities are obtained by differencing equation (5) as

$$\rho(I+1/2,J,N+1) = \rho(ID,J,N)*(1-DT/R(I+1/2)*(R(I+1)*U(I+1,J,N+1)-R(I)*U(I,J,N+1))/(R(I+1)-R(I)))$$

$$\rho(I,J+1/2,N+1) = \rho(I,JD,N)*(1-DT*(V(I,J+1,N+1)-V(I,J,N+1))/(Z(J+1)-Z(J)))$$

where

ID = 1 If U(I+1/2,J,N+1) GT 0
= I+1 If U(I+1/2,J,N+1) LT 0
JD = J If V(I,J+1/2,N+1) GT 0
= J+1 If V(I,J+1/2,N+1) LT 0.

This is the classical donor cell differencing technique. The most obvious advantages of this technique are its rigid numerical conservation and its stability. This scheme also insures that more material cannot be removed from a point than is present.

HULL has a continuous rezone capability. When this is employed, the interpolated velocities appearing in the mass flux equations are replaced by

$$U(I+1/2,J,N+1) - UR(I+1/2,J,N+1)$$

$$V(I,J+1/2,N+1) - VR(I,J+1/2,N+1)$$

where UR and VR are the interpolated grid velocities (determined arbitrarily by how fast one wishes to transport the coordinate grid). The corresponding momentum fluxes are

$$UF(I+1/2,J,N+1) = MF(I+1/2,J,N+1)*U(ID,J,N+1)$$

$$VF(I+1/2,J,N+1) = MF(I+1/2,J,N+1)*V(ID,J,N+1)$$

$$UF(I,J+1/2,N+1) = MF(I,J+1/2,N+1)*U(I,JD,N+1)$$

$$VF(I,J+1/2,N+1) = MF(I,J+1/2,N+1)*V(I,JD,N+1)$$

and the energy fluxes are

$$EF(I+1/2,J,N+1) = MF(I+1/2,J,N+1)*E(ID,J,N+1)$$

$$EF(I,J+1/2,N+1) = MF(I,J+1/2,N+1)*E(I,JD,N+1)$$

When these quantities are fluxed, final values for mass, density, velocity, and energy are computed by

$$M(I,J) = M(I,J,N)+MF(I-1/2,J,N+1)+MF(I,J-1/2,N+1)$$
$$-MF(I+1/2,J,N+1)-FM(I,J+1/2,N+1)$$

$$\rho(I,J) - M(I,J)/(\pi*(R(1+1/2)**2-R(I-1/2**2)*DZ(J))$$

$$U(I,J) = (U(I,J,N+1)*M(I,J,N)+UF(I-1/2,J,N+1)+UF(I,J-1/2,N+1)$$
$$-UF(I+1/2,J,N+1)-LF(I,J+1/2,N+1))/M(I,J)$$

$$V(I,J) = (V(I,J,N+1)*M(I,J,N)+EF(I-1/2,J,N+1)+EF(I,J-1/2,N+1)$$
$$-EF(I+1/2,J,N+1)-VF(I+1/2,J,N+1))/M(I,J)$$

$$I(I,J) = (E(I,J,N+1)*M(I,J,N)+EF(I-1/2,J,N+1)+EF(I,J-1/2,N+1)$$
$$-EF(I+1/2,J,N+1)-EF(I,J+1/2,N+1)-(U(I,J)**2+V(I,J)**2)$$
$$*M(I,J)/2)/M(I,J)$$

$$E(I,J) = I(I,J)+(U(I,J)**2+V(I,J)**2)/2$$

where the lack of a time specification indicates final values for this time step.

2. HULL: THE 3-DIMENSIONAL VERSION

The three-dimensional version of the HULL code solves the finite difference analogs of the system of partial differential equations describing inviscid, nonconducting fluid flow in the form

$$\frac{d\rho}{dt} + \rho\nabla \cdot \bar{u} = 0 \tag{18}$$

$$\rho \frac{du}{dt} + \nabla P = p\bar{g} \tag{19}$$

$$\rho \frac{dE}{dt} + \nabla \cdot P\bar{u} = \rho\bar{u} \cdot g \tag{20}$$

$$P = (\gamma-1)\rho I \tag{21}$$

where

ρ = material density (gm/cm^3)
P = pressure ($dynes/cm^2$)
$\bar{u}$ = (u,v,w) the fluid velocity (cm/sec)
$E = I + \frac{\bar{u}\cdot\bar{u}}{2}$ (ergs/gm)
I = internal specific energy (ergs/gm)
$\bar{g}$ = acceleration due to gravity (cm/sec^2)
t = time (sec.)
γ = specific heat at constant pressure divided by specific heat at constant volume

Equations (18) through (21) are solved in two phases. The first phase proceeds as a Lagrangian calculation insuring exact compliance with equation (18) when all mass points are properly transported. Choosing the following notation for the finite difference analogs of the above equation,

$$f(x_i,y_j,z_k,t_n) = f^n_{i,j,k}$$

and where subscripts on the left and right sides of the equations are suppressed on the right-hand side, the finite difference analogs of equations (19) and (20) in Cartesian three space with the z axis oriented in the direction of $\bar{g}$ are:

$$U^{n+1}_{i,j,k} = U^n - \frac{DT}{\rho^n DX}\left(P^{n+\frac{1}{2}}_{i+\frac{1}{2}} - P^{n+\frac{1}{2}}_{i-\frac{1}{2}}\right) \tag{22}$$

$$V^{n+1}_{i,j,k} = V^n - \frac{DT}{\rho^n DY}\left(P^{n+\frac{1}{2}}_{j+\frac{1}{2}} - P^{n+\frac{1}{2}}_{j-\frac{1}{2}}\right)$$

$$W^{n+1}_{i,j,k} = W^n - \frac{DT}{\rho^n DZ}\left(P^{n+\frac{1}{2}}_{k+\frac{1}{2}} - P^{n+\frac{1}{2}}_{k-\frac{1}{2}}\right) + DT \cdot G_k \tag{23}$$

$$\begin{aligned} E^{n+1}_{i,j,k} = E^n - \frac{DT}{\rho^n}\Big[&\left(P^{n+\frac{1}{2}}_{i+\frac{1}{2}} U^{n+\frac{1}{2}}_{i+\frac{1}{2}} - P^{n+\frac{1}{2}}_{i-\frac{1}{2}} W^{n+\frac{1}{2}}_{i-\frac{1}{2}}\right)/DX \\ &+ \left(P^{n+\frac{1}{2}}_{j+\frac{1}{2}} V^{n+\frac{1}{2}}_{j+\frac{1}{2}} - P^{n+\frac{1}{2}}_{j-\frac{1}{2}} V^{n+\frac{1}{2}}_{j-\frac{1}{2}}\right)/DY \\ &+ \left(P^{n+\frac{1}{2}}_{k+\frac{1}{2}} W^{n+\frac{1}{2}}_{k+\frac{1}{2}} - P^{n+\frac{1}{2}}_{k-\frac{1}{2}} W^{n+\frac{1}{2}}_{k-\frac{1}{2}}\right)/DZ\Big] \\ &+ DT \cdot V \cdot G_k \end{aligned} \tag{24}$$

where

$$DT = T^{n+1} - T^n$$
$$DX = X_{i+1} - X_i$$
$$DY = Y_{j+1} - Y_j$$
$$DZ = Z_{k+1} - Z_k$$

The time and space centered quantities are defined from the previous time step mesh quantities. In addition, we need pressure and velocity terms in the above equations and use an alternate form of the energy equation obtained from equations (19) and (20) for these;

$$\rho \frac{dI}{dt} + P\nabla \cdot \bar{u} = 0 \tag{25}$$

Solving equations (18), (21), and (25) for a constant gamma, we obtain

$$\frac{dP}{dt} + \gamma P \nabla \cdot \bar{u} = 0 \qquad (26)$$

The assumption of a constant gamma-law gas is not critical to the methodology since an effective $\gamma_{eff} = \frac{P}{\rho I} + 1$ can almost always be used since γ does not change significantly in a time step.

The finite difference analogs of equations (19) and (26) for the time and space centering quantities used in equations (22), (23), and (24) are:

$$U^{n+\frac{1}{2}}_{i+\frac{1}{2},j,k} = \frac{U^n_i + U^n_{i+1}}{2} - \frac{DT}{DX(\rho^{n+\frac{1}{2}}_i + \rho^{n+\frac{1}{2}}_{i+1})} (P^n_{i+1} - P^n_i) \qquad (27)$$

$$V^{n+\frac{1}{2}}_{i,j+\frac{1}{2},k} = \frac{V^n_j + V^n_{j+1}}{2} - \frac{DT}{DY(\rho^{n+\frac{1}{2}}_j + \rho^{n+\frac{1}{2}}_{j+1})} (P^n_{j+1} - P^n_j) \qquad (28)$$

$$W^{n+\frac{1}{2}}_{i,j,k+\frac{1}{2}} = \frac{W^n_k + W^n_{k+1}}{2} - \frac{DT}{DZ(\rho^{n+\frac{1}{2}}_k + \rho^{n+\frac{1}{2}}_{k+1})} (P^n_{k+1} - P^n_k) + \frac{DT\ G}{2}_{k+\frac{1}{2}} \qquad (29)$$

$$P^{n+\frac{1}{2}}_{i+\frac{1}{2},j,k} = \frac{P^n_i + P^n_{i+1}}{2} \left[(1 - \gamma \frac{DT}{2\ DX} (U^n_{i+1} - U^n_i) \right] \qquad (30)$$

$$P^{n+\frac{1}{2}}_{i,j+\frac{1}{2},k} = \frac{P^n_j + P^n_{j+1}}{2} \left[1 - \gamma \frac{DT}{2\ DX} (V^n_{j+1} - V^n_j) \right] \qquad (31)$$

$$P^{n+\frac{1}{2}}_{i,j,k+\frac{1}{2}} = \frac{P^n_k + P^n_{k+1}}{2} \left[1 - \gamma \frac{DT}{2\ DZ} (W^n_{k+1} - W^n_k) \right] \qquad (32)$$

The G terms in equations (23), (24), and (29) are calculated by solving the hydrostatic equations on the finite difference mesh at the appropriate mesh interval. (An automatic program abort occurs if this calculated value of G ever differs from the correct theoretical value at the current altitude by more than 1 percent.)

The above set of finite difference equations is second order accurate for a fixed mesh interval and is reasonably well-behaved when adjacent cells are within 10 percent of one another in size.

Normally, a Lagrangian solution of equations (18), (19), and (20) requires the transport of vertices. In the three-dimensional mesh we choose instead to flux across cell boundaries while conserving energy, momentum and mass. Although this is the main source of entropy production in the method, it has the advantage of providing sufficient dissipation to permit calculation of strong shocks without the difficulty of managing an explicit viscosity term.

In addition, a continuous rezone is overlayed on the flux scheme. In three-dimensions it is necessary to alternate the application of rezone velocities so that only one cell boundary is moved during a given time step. This requirement arises due to accumulation of second and higher order errors in ambient zones which can upset hydrostatic equilibrium.

By solving equation (18) we obtain the material density to be fluxed. Taking account of dilatational terms in all three directions simultaneously in a straightforward manner leads to instability in regions of rapid expansion. A method of first order accuracy but of superior stability characteristics can be obtained by solving for the dilatational terms one coordinate at a time, and since, if stability conditions are adhered to, the eigenvalues of each of the finite difference operators are less than unity, then their products will also be less than one. This leads to

$$\tilde{\rho}_{i+\frac{1}{2},j,k} = \rho^n_{id}/\Delta\bar{w}_i \tag{33}$$

$$\tilde{\rho}_{i,j+\frac{1}{2},k} = \rho^n_{jd}/\Delta\bar{u}_j \tag{34}$$

$$\tilde{\rho}_{i,j,k+\frac{1}{2}} = \rho^n_{kd}/\Delta\bar{u}_k \tag{35}$$

The d following a cell index indicates the donor cell values are used. Also,

$$\Delta\bar{u}_{i,j,k} = \left[1 + \frac{DT}{DX}\left(U^{n+1}_{i+1} - U^n_i\right)\right] \cdot \left[1 + \frac{DT}{DY}\left(V^{n+1}_{j+1} - V^n_j\right)\right] \cdot \left[1 + \frac{DT}{DZ}\left(W^{n+1}_{k+1} - W^n_k\right)\right] \tag{36}$$

The effect of this apparently ad hoc treatment is to drastically reduce the rather bothersome corner-coupling difficulties which often result in spherical features such as fireballs being "squared-off." We also found that we can run the code at about 0.9 of the usual one-dimensional Courant condition, an obvious computational speed advantage.

SECTION IV

EXPERIMENTAL AND THEORETICAL COMPARISONS

This section compares some theoretical calculations using HULL (and its predecessor, SHELL) with various high explosive (HE) experimental data. The AFWL has provided air blast calculations in support of nearly all large scale HE detonations beginning with the DISTANT PLAIN series and continuing through DICE THROW (refs. 4 through 12). Hence, there exists a wealth of data for comparisons with theoretical calculations.

Figure 1 is a comparison of the overpressure versus ground range for a 500 ton tangent sphere of TNT. This calculation was made with our version of the SHELL code (ref. 6), which now has been replaced by the HULL code at the AFWL. Note that although SHELL results fall below the experimental data below pressures of about 10 psi, HULL results are considerably improved over those from SHELL in that pressure regime. Experimental results are plotted from PRARIE FLAT (ref. 9) and DIAL PACK which were both detonated at Suffield, Canada.

MINE UNDER (refs. 5 and 10) was a 100 ton TNT sphere detonated 1 diameter above the ground. Agreement for the peak overpressure versus ground range between calculation and experiment was similar to that of the tangent sphere case. Positive phase duration (fig. 2) is somewhat more difficult to measure experimentally than is peak overpressure. This is reflected in the relatively large experimental error bars.

Figures 3 through 6 compare several parameters measured during MIXED COMPANY, a 500 ton tangent sphere of TNT detonated near Grand Junction, Colorado, with AFWL calculations. Measurements were made by Ballistics Research Laboratory (BRL) and the Civil Engineering Division of the AFWL. Calculations were made by the AFWL Technology Division.

The peak overpressure is in good agreement as usual. The overpressure impulse (fig. 4), although somewhat more difficult to measure, appears to be in good agreement. As mentioned previously the positive duration is very difficult to measure, and is reflected by the large amount of experimental scatter.

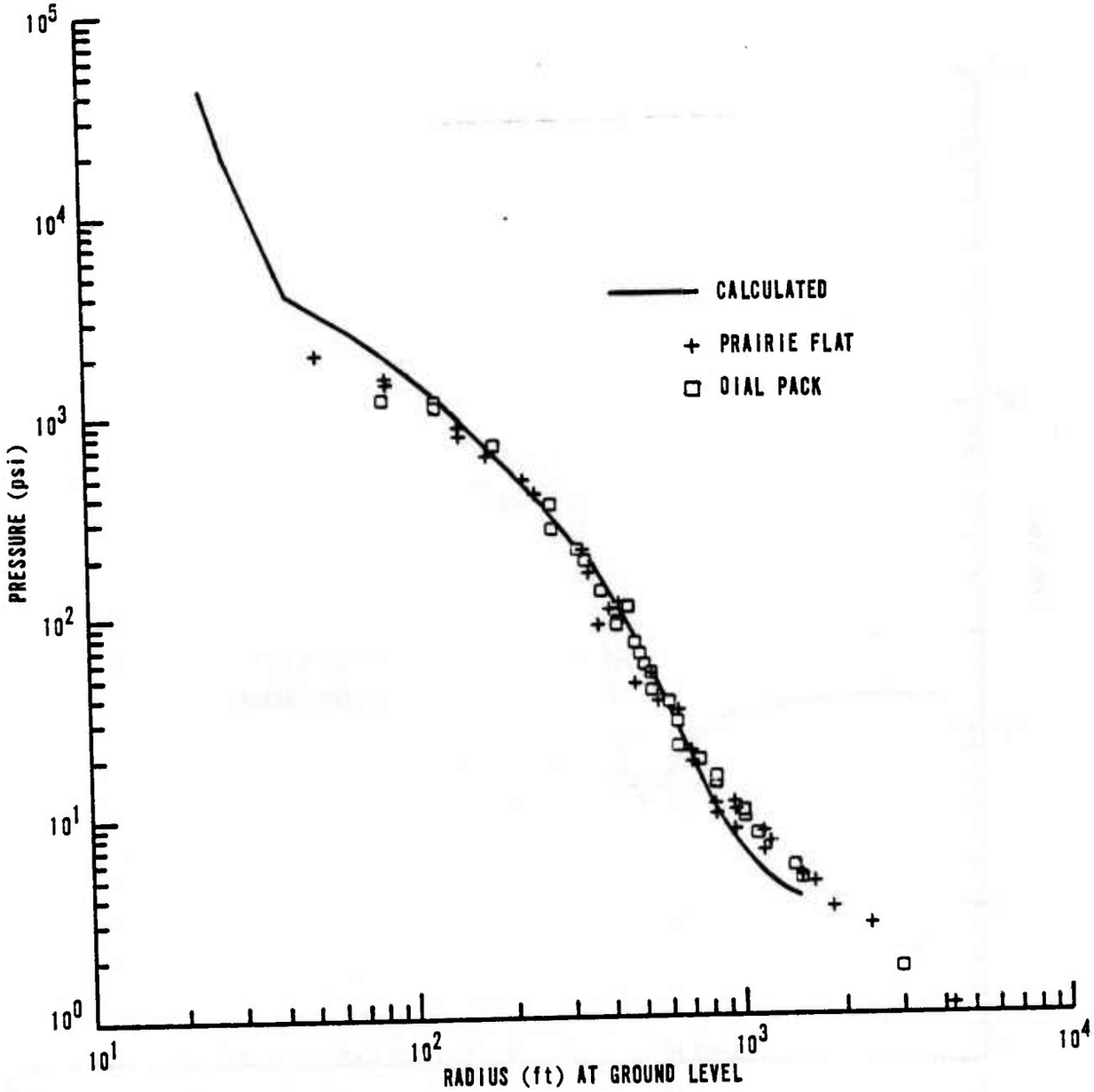

Figure 1. DIAL PACK (overpressure versus radius)

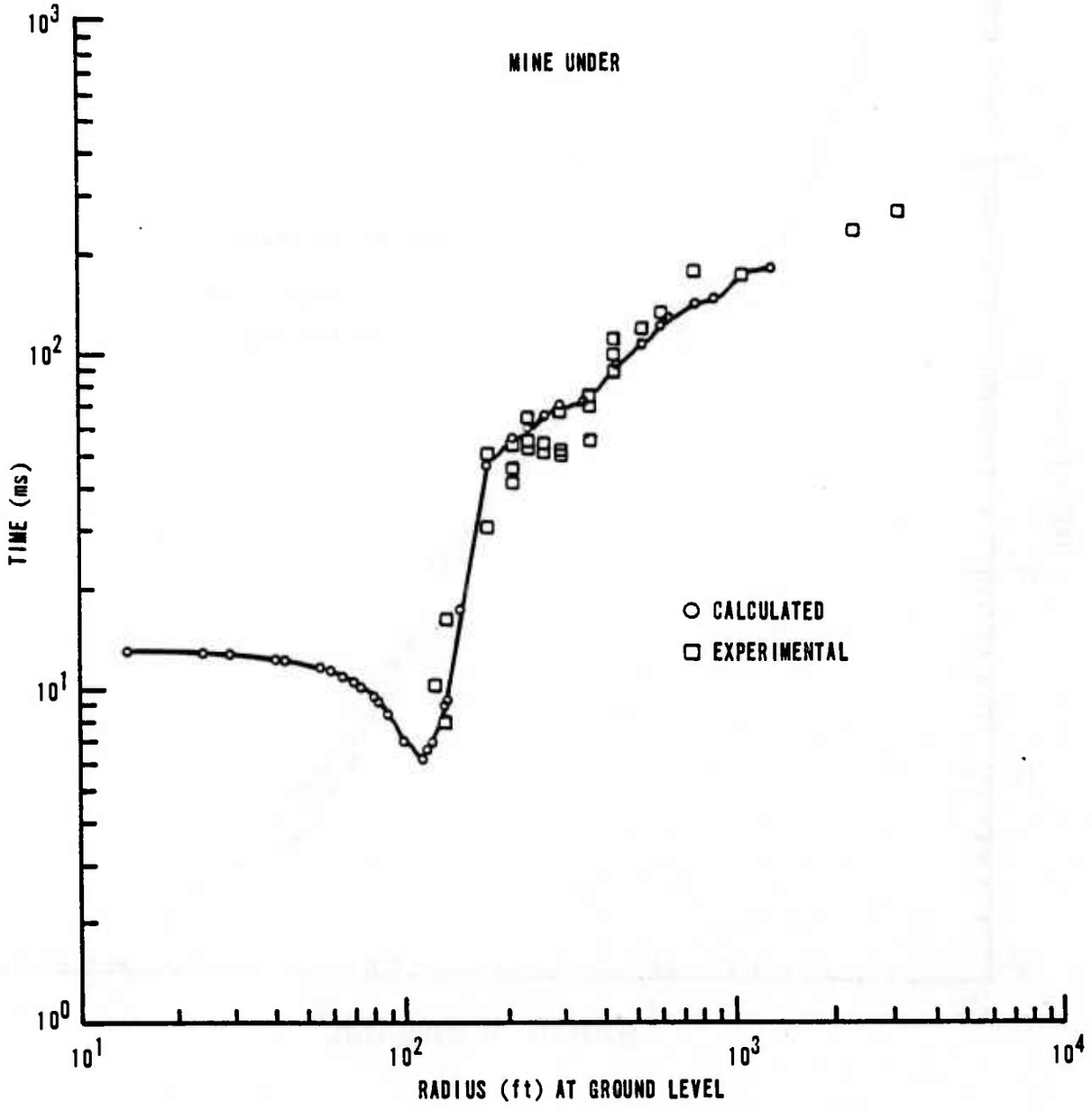

Figure 2. Positive Phase Duration Versus Radius

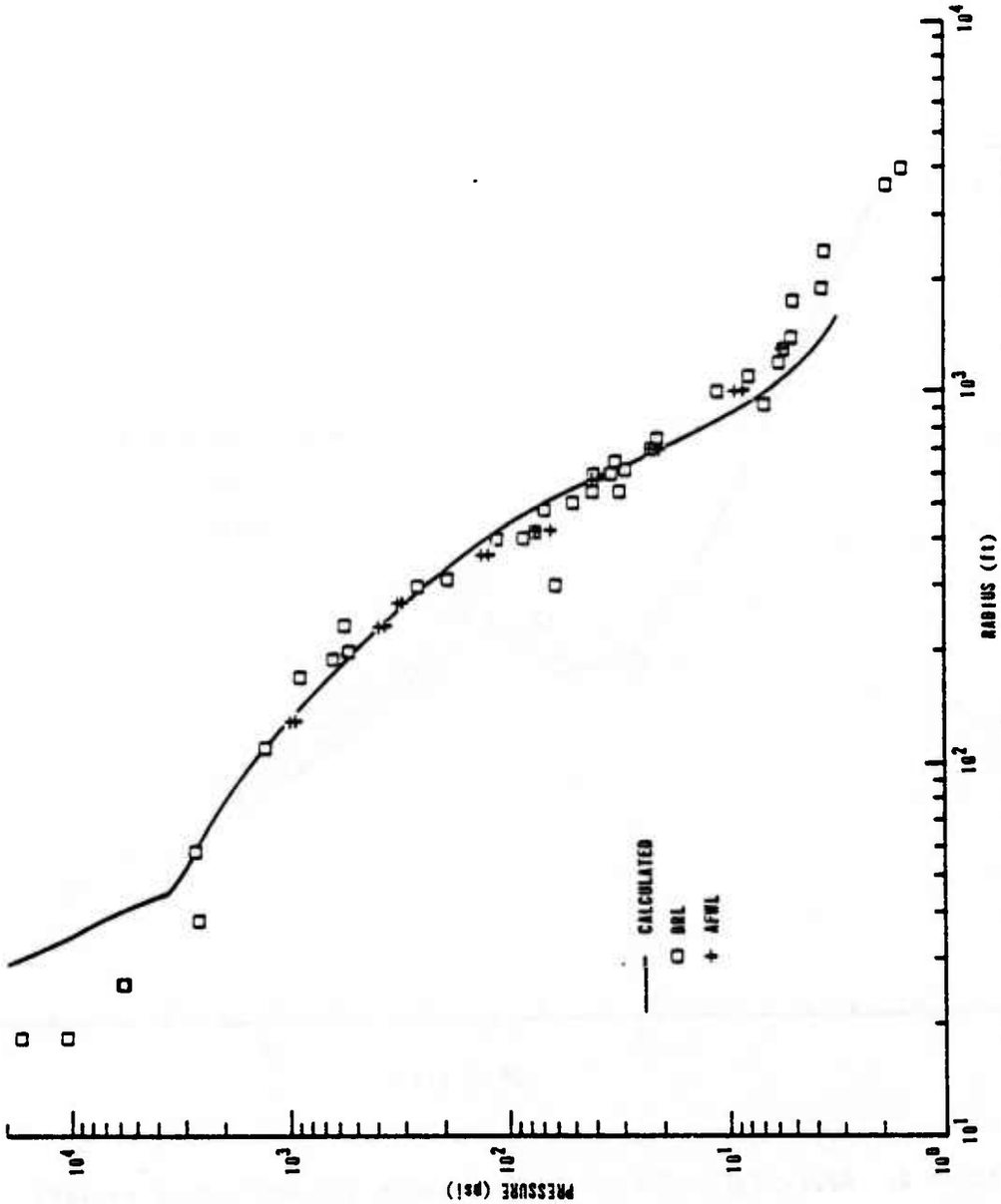

Figure 3. AFWL-MIXED COMPANY (overpressure versus radius)

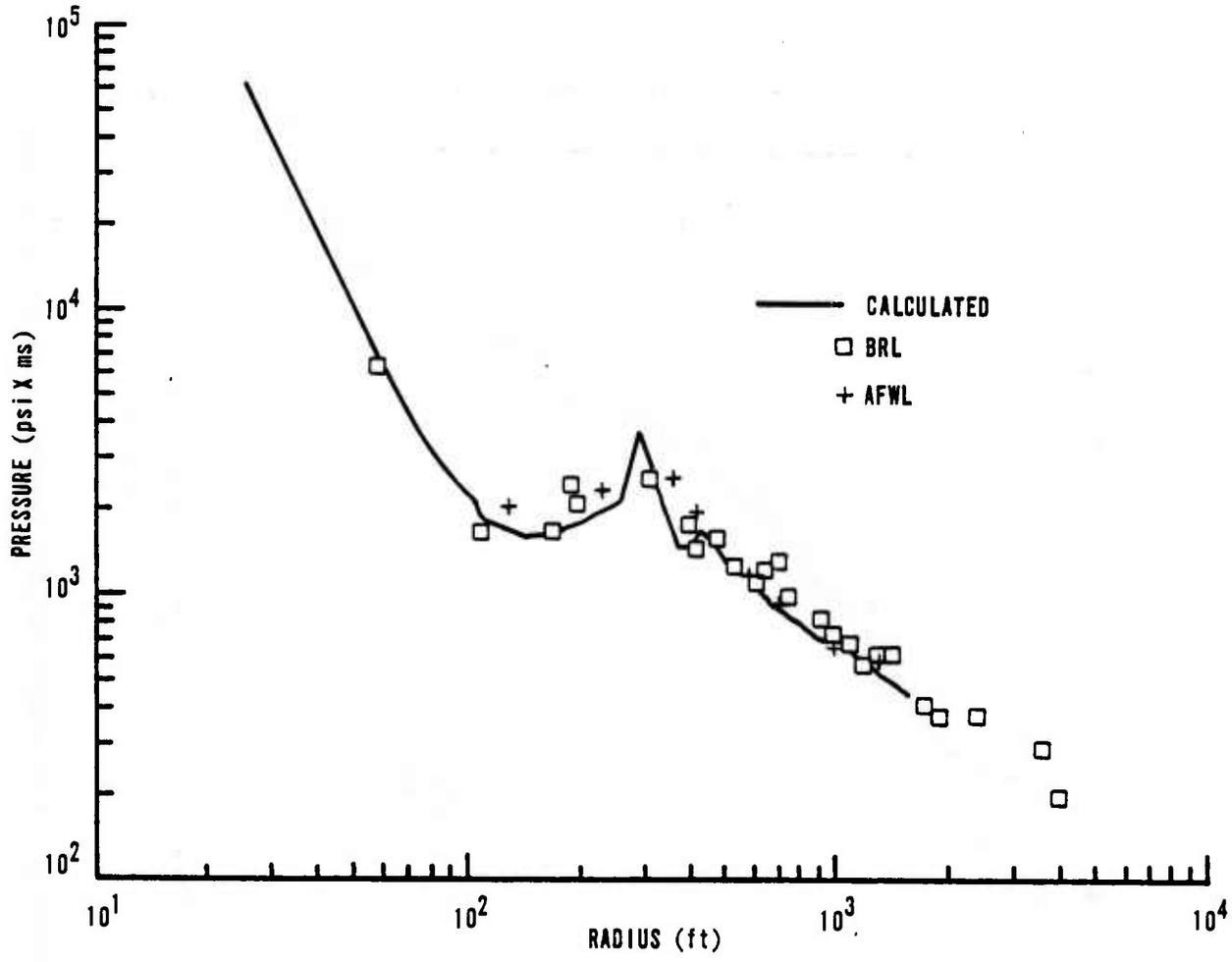

Figure 4. AFWL-MIXED COMPANY (overpressure impulse versus radius)

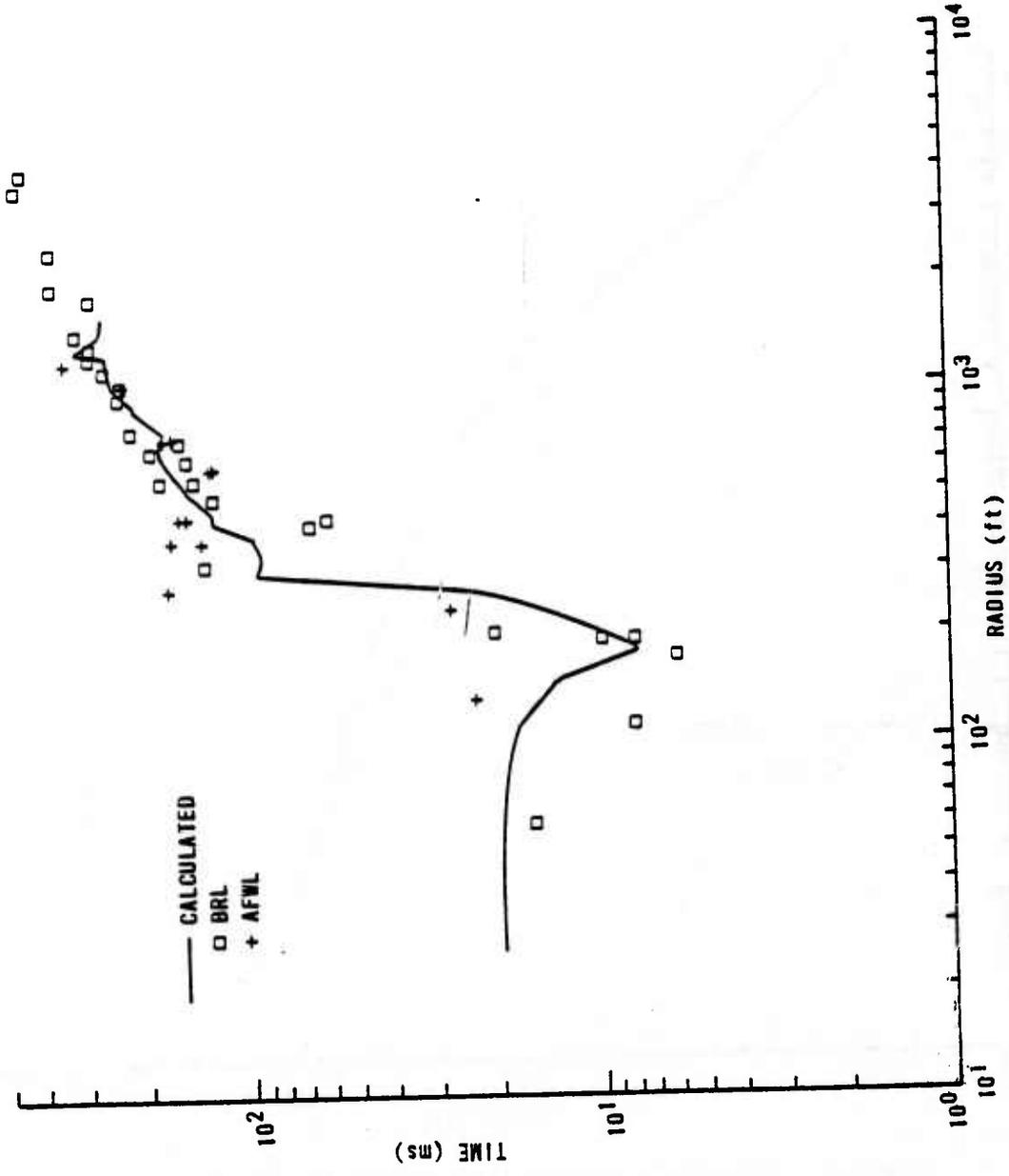

Figure 5. AFWL-MIXED COMPANY (positive phase duration)

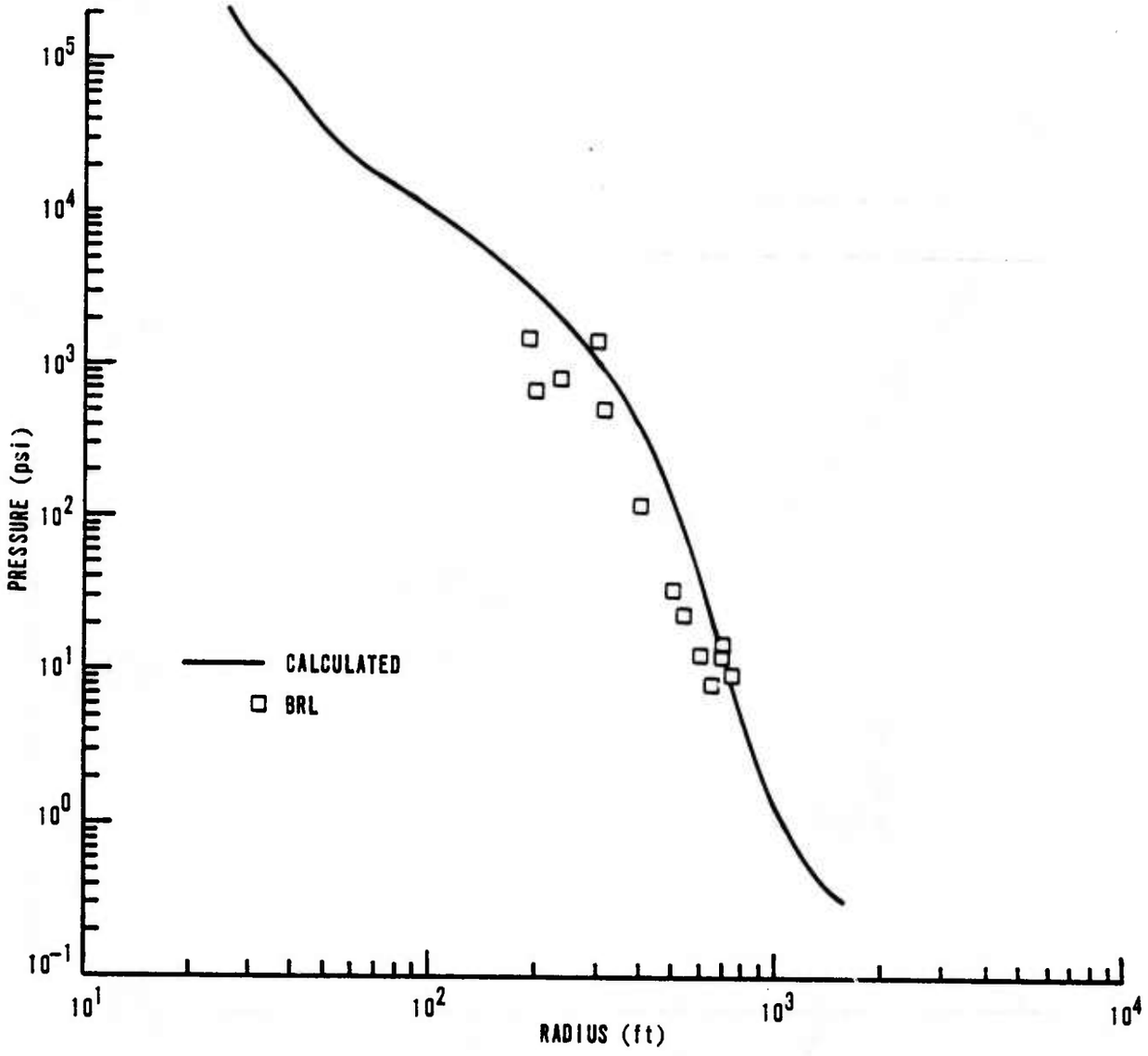

Figure 6. AFWL-MIXED COMPANY (horizontal dynamic pressure)

Considerable comment has been made regarding the theoretical capability to properly calculate dynamic pressure. From the conservation laws of mass, momentum and energy one can infer that if one parameter at the shock front is known, all other parameters are uniquely determined. Since the codes solve the conservation equations, it is argued that when the overpressure is being accurately calculated, the dynamic pressure must also be accurately calculated.

Because dynamic pressure cannot be measured directly with present instrumentation, the method used is to measure the total pressure and the overpressure at the same point. The dynamic pressure is calculated by making a point by point comparison of the two measured waveforms. This can lead to accentuated differences; and, therefore, several smoothing techniques are used to attempt to damp resulting oscillations.

In addition to the usual difficulties mentioned above, the MIXED COMPANY (ref. 12) total pressure gages were 3 feet above ground, whereas the overpressure was measured at ground level. The calculations indicate a significant pressure gradient between ground level and 3 feet. This would lead to lower "measured" dynamic pressure. Figure 6 shows, in general, this lowering of the peak dynamic pressure.

Figures 7 through 14 compare calculated and experimental results for Dipole West (ref. 26), shots 8 through 11. These experiments used two charges detonated one above the other such that the distance between charges was twice that of the lower charge above the ground. Thus, direct comparisons could be made between real and ideal surfaces and calculations. Shots 8 and 11 had a height of burst of 25 feet (50 feet charge separation), the ground surface was smooth for shot 8 and had approximately 1 foot corrugations in shot 11. The experimental data in figure 7 are for the real surface only; the calculation falls between the arrival times for the rough and smooth surfaces.

Figure 8 is a comparison of the overpressure peaks. The calculation falls low by about 10 percent at ground zero but by a distance of 10 feet has regained the peak and falls within experimental scatter. These calculations were run with the HULL code; note that the overpressure peak agreement at 10 psi is excellent when compared to the smooth surface. The rough surface has slightly enhanced the overpressure peak at low overpressure.

Figure 9 shows the effect of decreasing the height of burst from 25 to 15 feet. The flattening of the curve near 100 feet is caused by the reflected

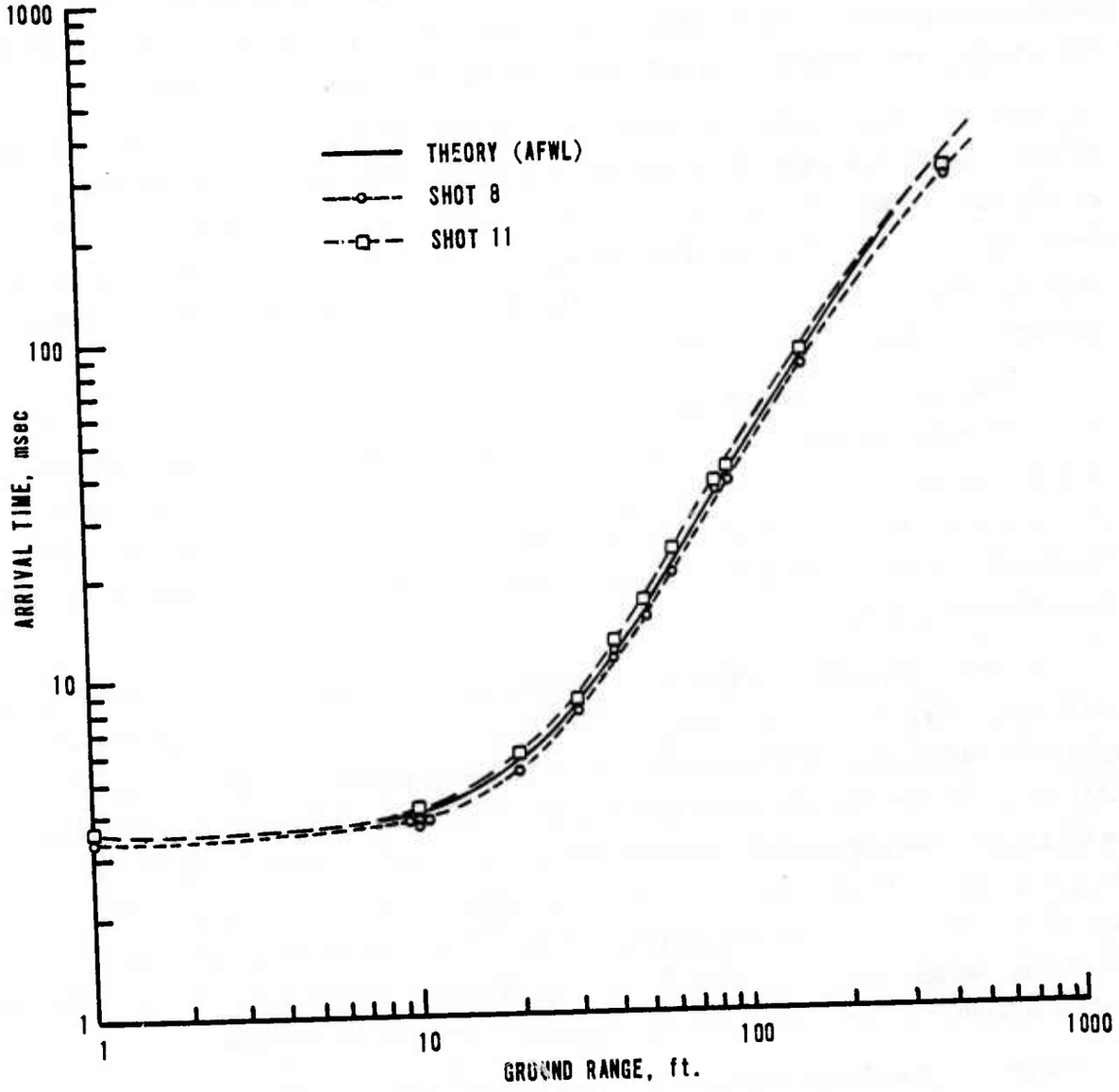

Figure 7. Comparison of Calculated and Experimental Arrival Times at Ground Level; Shots 8 and 11, Dipole West, (extracted from ref. 26, p. 205)

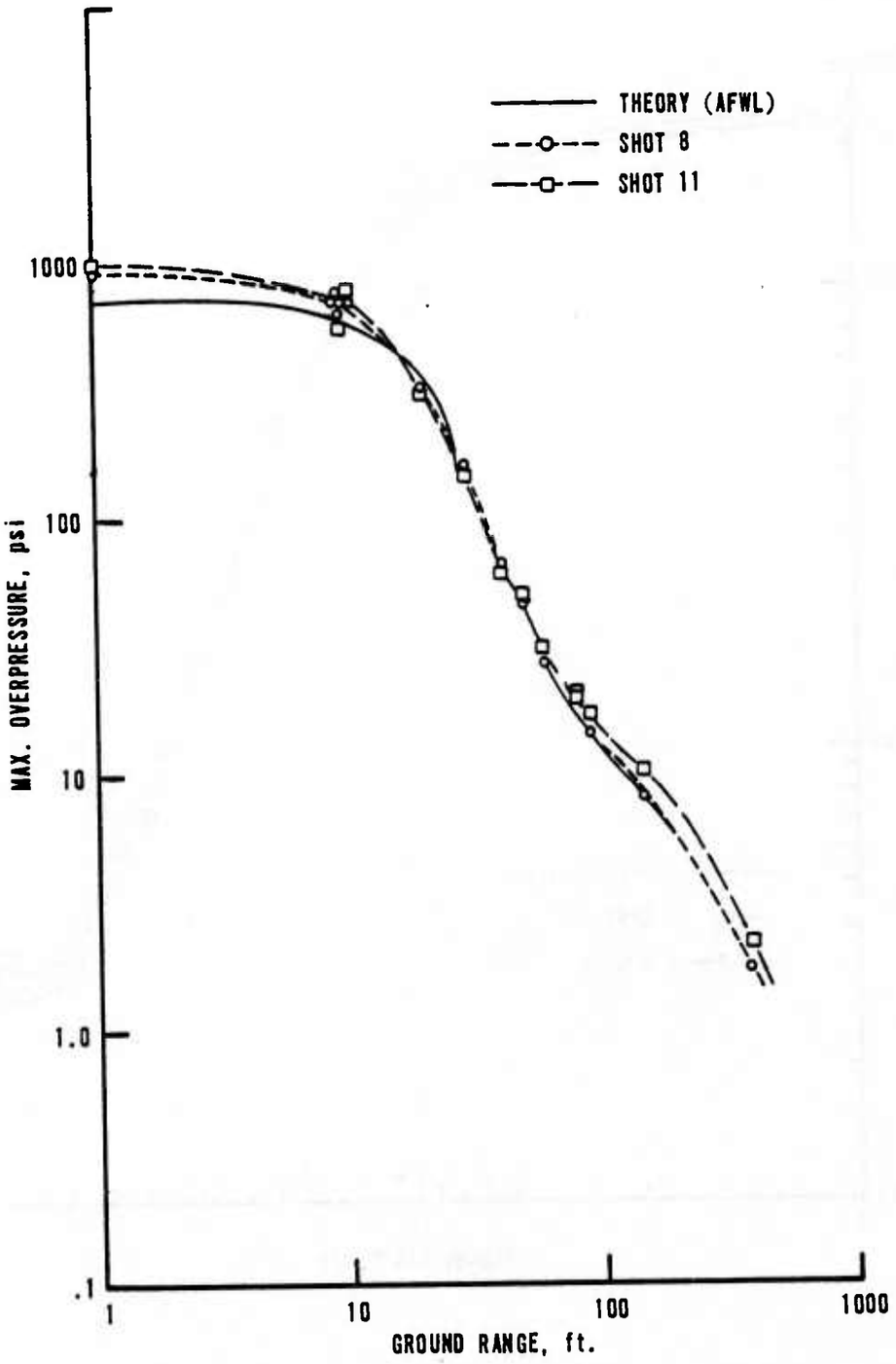

Figure 8. Comparison of Calculated and Experimental Maximum Overpressures at Ground Level; Shots 8 and 11, Dipole West, (extracted from ref. 26, p. 203)

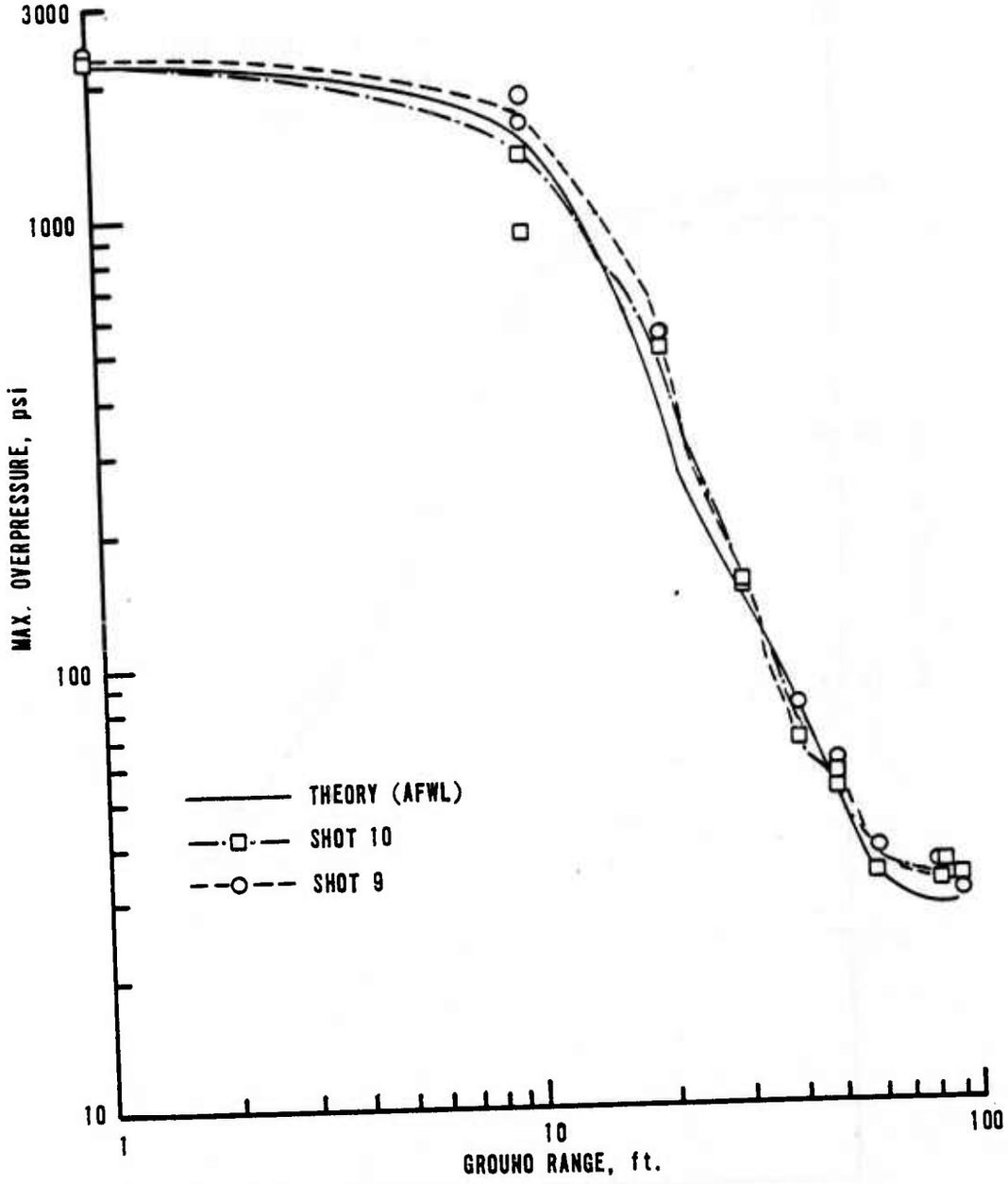

Figure 9. Comparison of Calculated and Experimental Maximum Overpressures at Ground Level; Shots 9 and 10, Dipole West, (extracted from ref. 26, p. 213)

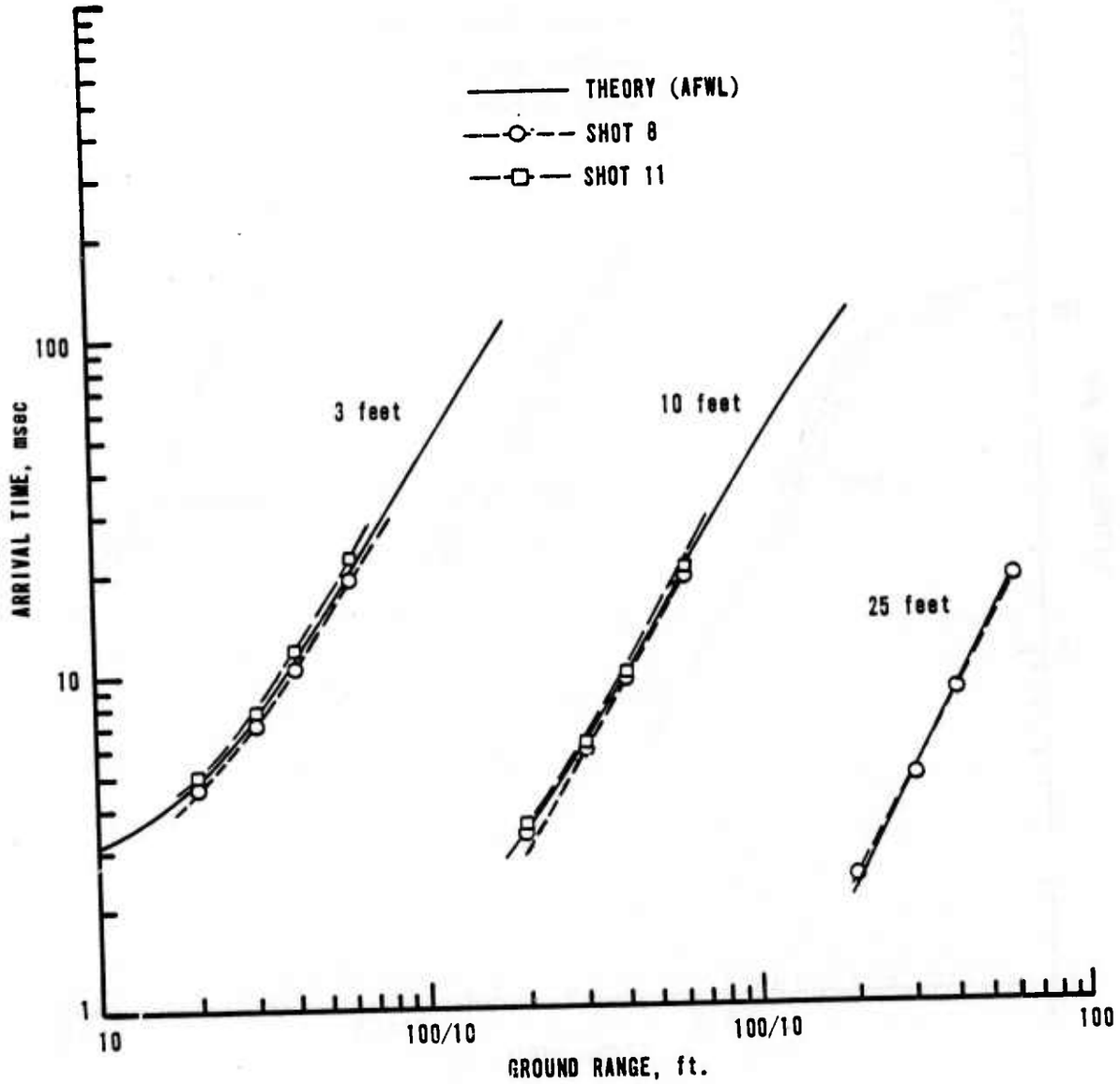

Figure 10. Comparison of Calculated and Experimental Arrival Times at 3, 10 and 25 Feet; Shots 8 and 11, Dipole West, (extracted from ref. 26, p. 206)

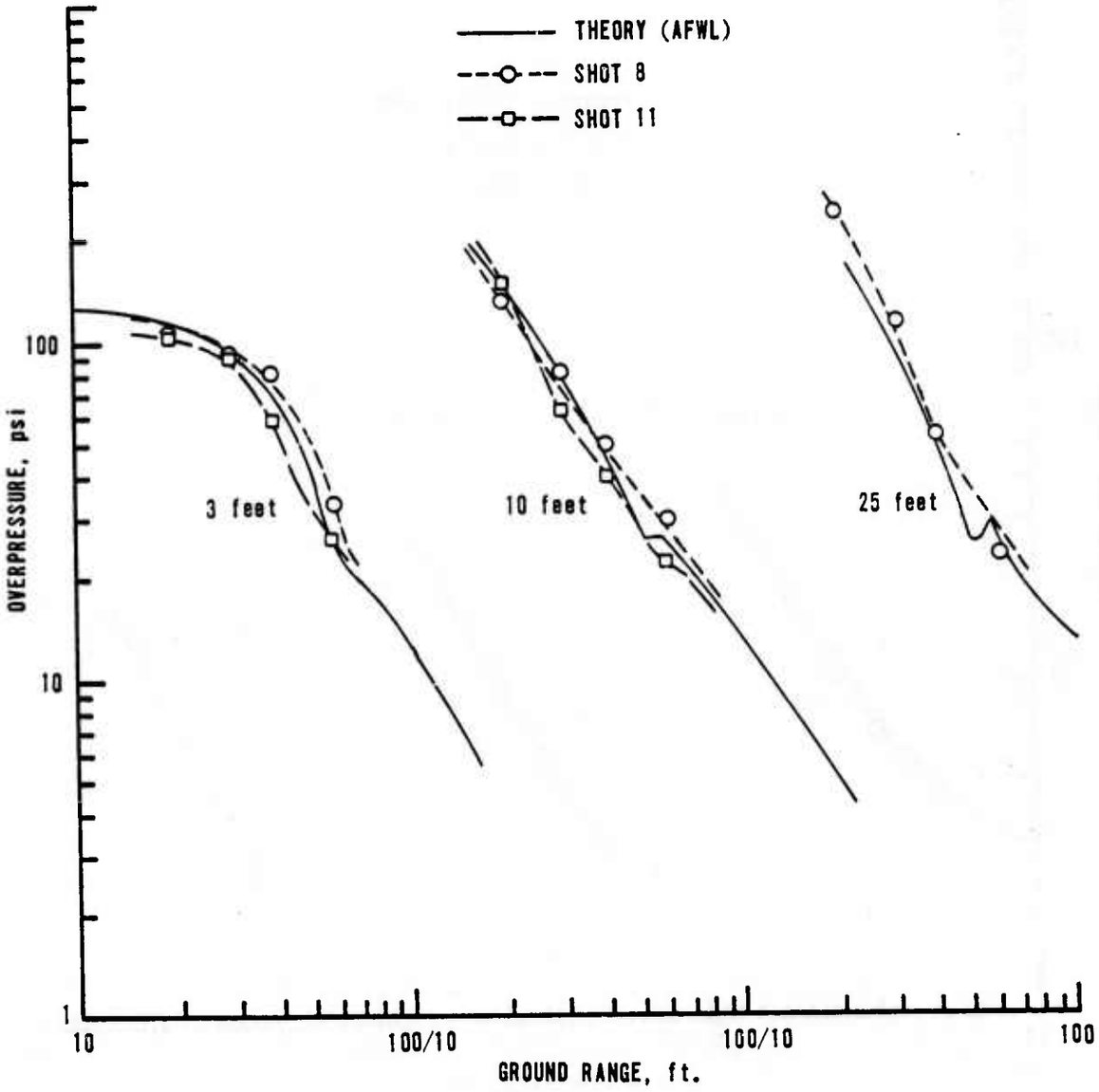

Figure 11. Comparison of Calculated and Experimental Maximum Overpressures at 3, 10, and 25 Feet; Shots 8 and 11, Dipole West, (extracted from ref. 26, p. 204)

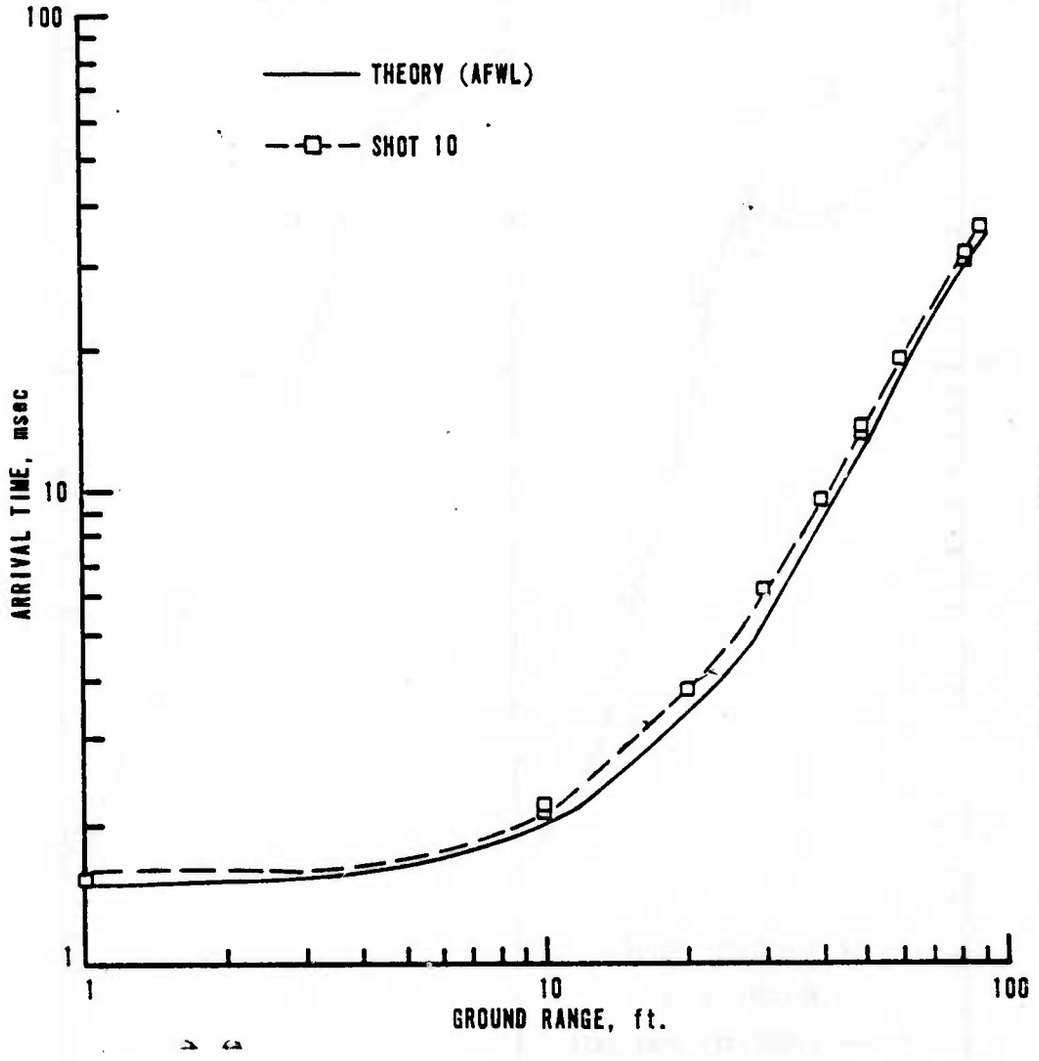

Figure 12. Comparison of Calculated and Experimental Arrival Times at Ground Level; Shot 10, Dipole West, (extracted from ref. 26, p. 215)

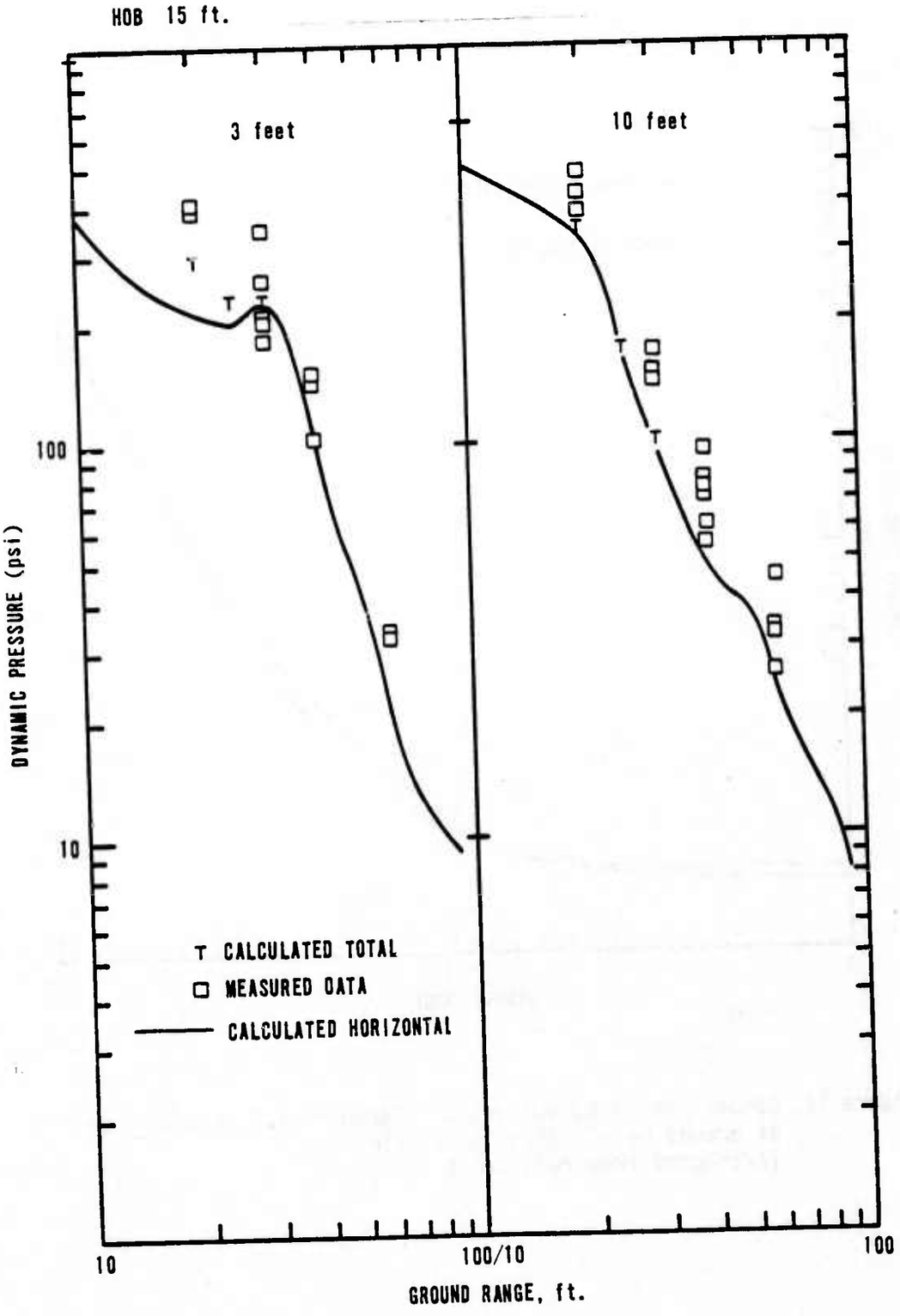

Figure 13. Dipole West (dynamic pressure)

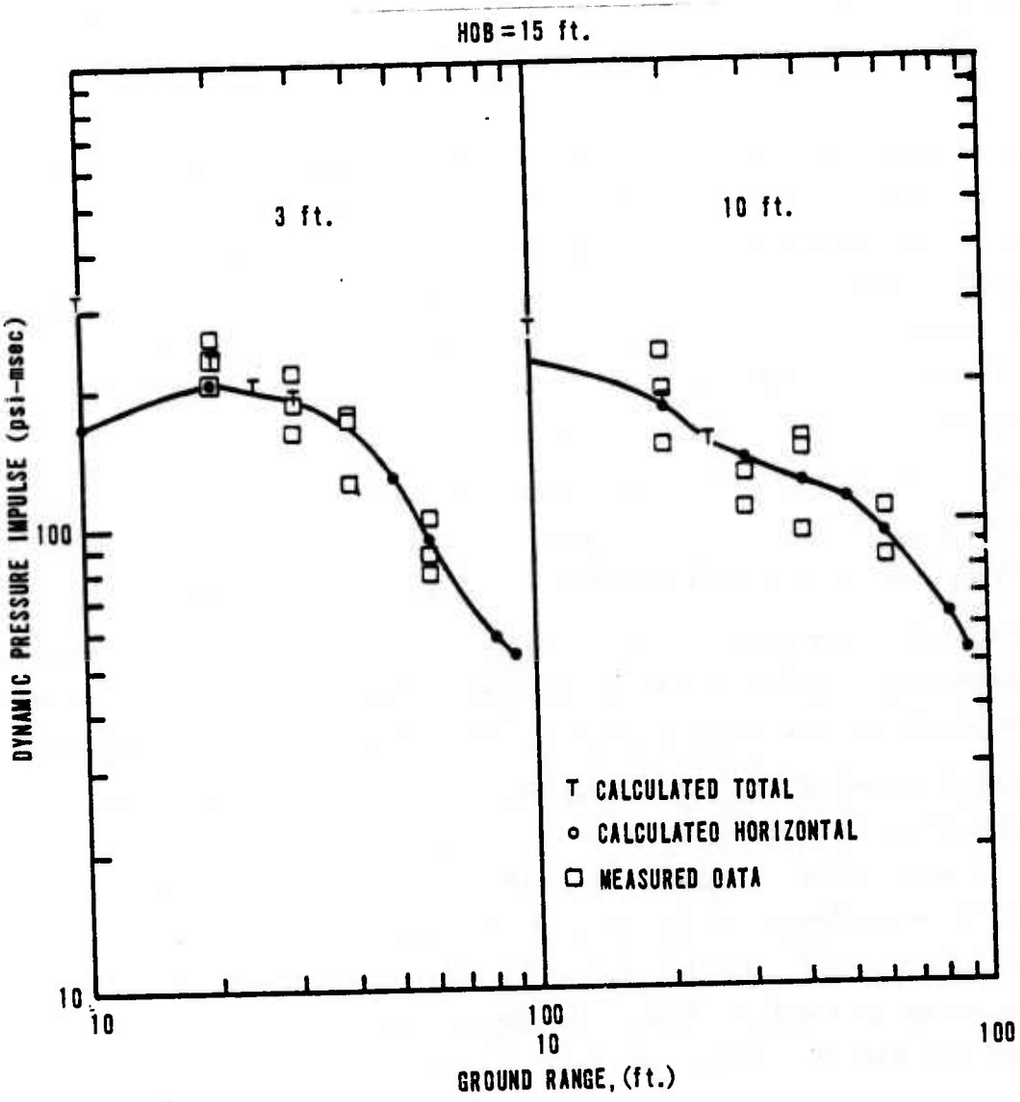

Figure 14. Dipole West (dynamic pressure impulse)

shock from the second burst catching that of the first. Again, the calculation falls within 5 percent of the experimental curves.

Figures 10 and 11 are for gages mounted 3, 10, and 25 feet above the ground surface. This demonstrates that the calculations are handling the entire flow field properly, not just a small region near the ground.

Figure 12 clearly shows the slowing of the shock front by the real surface compared to the ideal used by the calculation. The maximum difference is about 2 percent.

Dipole West (ref. 26) measurements for dynamic pressure were also made. The significant difference here is that the total pressure and overpressure were measured at the same ground range and at the same height above the ground. The peak dynamic pressure data (fig. 13) has a relatively large amount of scatter for the reasons mentioned earlier. The integrated dynamic pressure has the effect of smoothing individual oscillations, thus reducing the scatter and agreeing much better with the calculations (fig. 14).

Some of the most carefully performed experiments in recent years were made by Carpenter at TRW (ref. 27). A large number of triply redundant detonations of PBX-9404 spheres were exploded over a polished concrete slab.

Calculations were made by the Technology Division of the AFWL in support of this project. Figures 15 and 16 show that although the code is missing the absolute peaks the integrated waveforms (impulse) show excellent agreement.

The most recent HE tests have been those of PRE DICE THROW. Event 2 was a 6 ton detonation of a capped cylinder of AN/FO. The HULL calculation required not only a never before calculated geometry but a relatively unknown explosive. Figure 17 is a comparison of the experimental and calculated overpressure peaks. Agreement is excellent. In this particular experiment, waveform comparison of actual measured data was possible. The comparison showed that the calculated waveforms were virtual overlays of those measured.

It has been the intent of this section to acquaint the reader with the accuracy of the methods employed in theoretical air-blast calculations performed at the AFWL by presenting a wide variety of experimental data compared with calculated results. In nearly all cases discrepancies between calculations and experiments can be understood in terms of minor shortcomings of the experimental or calculational technique. In no case are any of the remaining discrepancies considered serious.

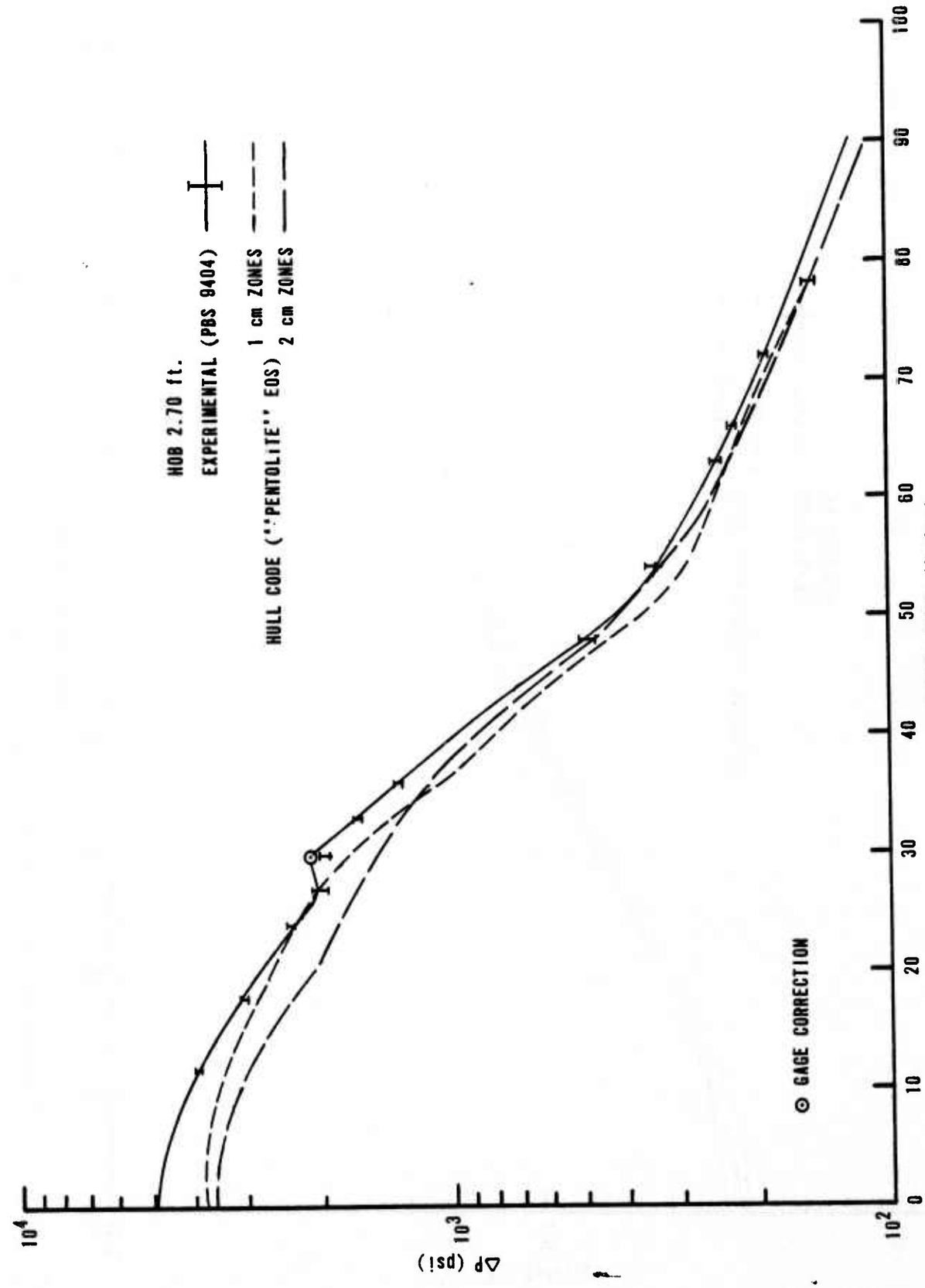

Figure 15. Surface Overpressure versus Ground Range for 8 LB HE Spheres

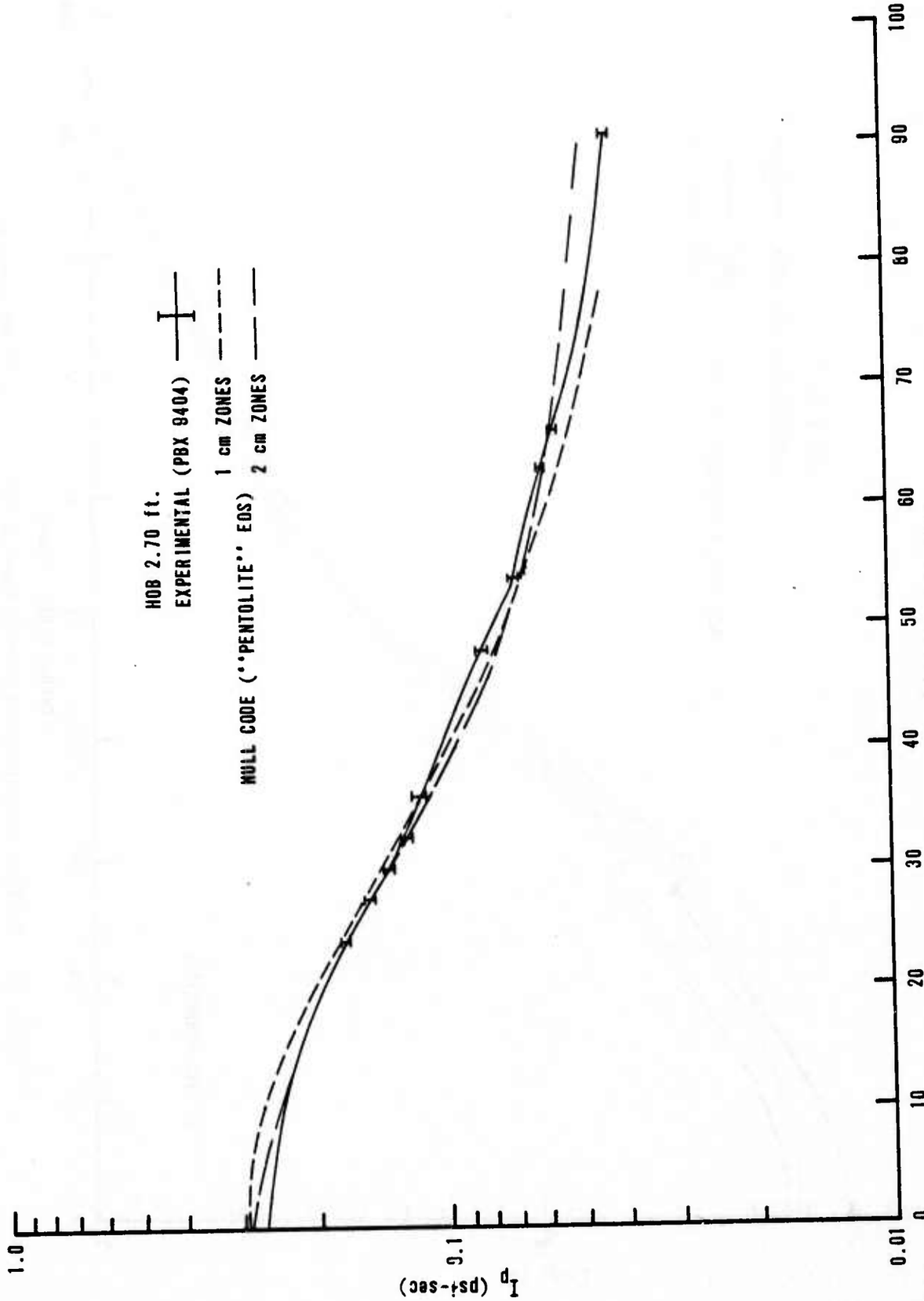

Figure 16. Positive Phase Impulse versus Ground Range for 8 LB HE Spheres

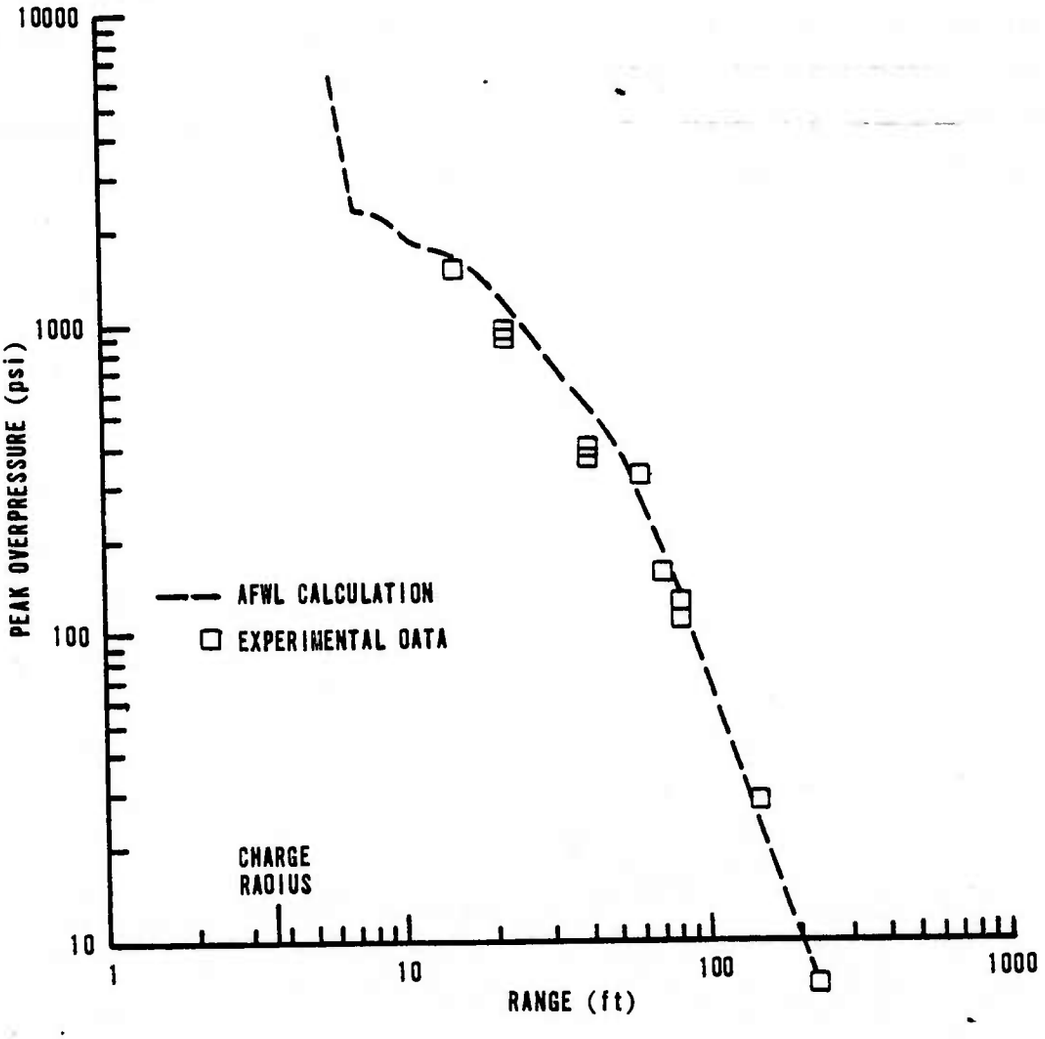

Figure 17. PRE DICE THROW 1 Calculation (Event 2)

The large variety of calculations of air blast indicates that the large scale hydrocode is a reliable method of predicting all phases of shock propagation from source to a few psi. The HULL code has been used to calculate the blast phenomenology from high explosive sources ranging from 8 pounds to 500 tons. With few exceptions the calculational results are in excellent agreement with experimental data. Calculations of blast from nuclear detonations are somewhat easier to make than those involving high explosives because the large mass of detonation products is not present. The calculation must be concerned with only one material, air, which is well understood. On this basis, we expect the results of nuclear blast calculations to be at least as accurate (if not more so) as those for high explosives.

REFERENCES

1. Evans, M.W., and Harlow, F.H., The Particle-In-Cell Method for Hydrodynamic Calculations, LA-2139, Los Alamos Scientific Laboratory, 1957.

2. Johnson, W.E., OIL A Continuous Two-Dimensional Eulerian Hydrodynamic Code, GAMD-5580, General Atomic Division, General Dynamics Corporation, 1965.

3. Nawrocki, E.A., et al., Private communication.

4. Nawrocki, E.A., Theoretical Calculations of DISTANT PLAIN Events, in DASA 1947-1, 1967.

5. Needham, C.E., Theoretical Air Blast Calculation, in DASA 1947-1, 1967.

6. Whitaker, W.A., Nawrocki, E.A., Needham, C.E., Troutman, W.W., Theoretical Calculations of the Phenomenology of HE Detonations, AFWL-TR-66-141, Air Force Weapons Laboratory, 1966.

7. Nawrocki, E.A., Whitaker, W.A., Needham, C.E., Theoretical Calculations of the Phenomenology of DISTANT PLAIN Event 6, AFWL-TR-67-57, Air Force Weapons Laboratory, 1967.

8. Needham, C.E., Nawrocki, E.A., Whitaker, W.A., Theoretical Calculations of the Detonation of a 1000 Pound Sphere of TNT at 15 Feet Above Ground Level, AFWL-TR-66-128, Air Force Weapons Laboratory, 1966.

9. Needham, C.E., PRAIRIE FLAT Air Blast Calculations, AFWL-TR-69-4, Air Force Weapons Laboratory, 1969.

10. Needham, C.E., and Burghard, T.H., Air Blast Calculations Event MINE UNDER, AFWL-TR-69-105, Air Force Weapons Laboratory, 1969.

11. Needham, C.E., A Code Method for Calculating Hydrodynamic Motion in HE Detonations, Proceedings Fifth Symposium on Detonation, ACR-184, Office of Naval Research, 1970.

12. Needham, C.E., Project LN103 - Theoretical Air Blast Calculations, DNA 3151P1, Defense Nuclear Agency, 1973.

13. Whitaker, W.A., et al., Private communication.

14. Needham, C.E., and Clemens, R.W., Recent Calculations on Cloud Dynamics and Particle Trajectories, WLTT-TN-70-10, Air Force Weapons Laboratory, 1970.

15. Ganong, G.P., and Roberts, W.A., The Effect of the Nuclear Environment on Crater Ejecta Trajectories for Surface Bursts, AFWL-TR-68-125, Air Force Weapons Laboratory, 1968.

REFERENCES (Continued)

16. Whitaker, W.S., et al., Private communication.

17. Ganong, G.P., et al., Private communication.

18. Ganong, G.P., and Whitaker, W.A., The Nuclear Blast Precursor, AFWL-TR-69-19, Air Force Weapons Laboratory, 1969.

19. Needham, C.E., Theoretical Calculations for a Precursor Simulation, AFWL-TR-67-140, Air Force Weapons Laboratory, 1968.

20. Whitaker, W.A., et al., Private communication.

21. Durrett, R.E., et al., Private communication.

22. Reynolds, R.C., SPSHELL, OILDROP, and SPCLAM: Three Programs to Solve Hydrodynamics Problems in Two Dimensions, AFWL-TR-70-96, Air Force Weapons Laboratory, December 1970.

23. Leigh, G.G., A Calculation of the Blast Wave from the Constant Velocity Detonation of an Explosive Sheet, AFWL-TR-71-137, Air Force Weapons Laboratory, November 1971.

24. Whitaker, W.A., Durrett, R.E., and Clemens, R.W., SHELL for the ILLIAC IV, AFWL-TR-72-33, Air Force Weapons Laboratory, March 1972.

25. Proceedings of Eric H. Wang Symposium on Protective Structure, July 1970.

26. Keefer, Reisler, Multiburst Environment-Simultaneous Detonations, Project Dipole West, BRL Report No. 1766, March 1975.

27. Height of Burst Blast Effects at High Overpressures, DNA 3437F, Defense Nuclear Agency, October 1974.

DISTRIBUTION

No. cys	
	AFATL, Eglin AFB, FL 32554
1	Maj D. Matuska
1	Maj R. Durrett
	Stanford Research Institute
	333 Ravenswood AV
	Menlo Park, CA 94025
1	Dr. W. Chestnut
1	Dr. Allan Burns
1	Dr. Georgellen Smith
	JSTPS/JPS, Offutt AFB, NE 68113
1	Capt D. Goetz
	Euclid Research Group
	1760 Solano Ave
	Berkeley, CA 94707
1	Ian O. Huebsch
	HDSAC/XOBM, Offutt AFB, NE 68113
1	LtCol Kelley
1	SAMSO/MNNH, Norton AFB, CA 92409
	Hq USAF, Wash, D C 20330
1	SA
1	SAMI
1	PREE
1	PREPB
1	RDQPN, 1D425
1	Hq USAF, AFTAC/TAP, Patrick AFB, FL 32925
1	AFCEC/PREC, Tyndall AFB, FL 32401
	AFISC, Norton AFB, CA 92409
1	PQAL
1	SE
	AFSC, Andrews AFB, Wash D C 20334
1	DOB
1	DLSP
1	XRP
1	T&E

No. cys	
	TAC, Langley AFB, VA 23365
1	DEE
1	DERP
1	LGMD
	CINCSAC, Offutt AFB, NE 68113
1	DEE
1	DOXS
1	XPFC
	ADC, Ent AFB, CO 80912
1	DOA
1	XPQDQ
1	XPQY
1	AUL(LDE), Maxwell AFB, AL 36112
1	AU (ED, DIR CIV ENG), Maxwell AFB, AL 36112
	AFIT, WPAFB, OH 45433
1	Tech Lib, Bldg 640 Area B
1	CES
	CINCUSAFE, APO New York 09012
1	DOA
1	USAF, SCLO (Maj Pierson, Ch, LO) POB 348 Toronto, ON, Canada M5K 1K7
	USAFA, CO 80840
1	DFSLB
1	FJSRL, CC
1	DFCE
	AFML, WPAFB, OH 45433
1	Tech Lib
	AFAL, WPAFB, OH 45433
1	TE
	AFFDL, WPAFB, OH 45433
1	(DOO/Lib)

DISTRIBUTION (cont'd)

No. cys	
	AFAPL, WPAFB, OH 45433
1	(Tech Lib)
	ASD, WPAFB, OH 45433
1	(Tech Lib)
1	(DEE)
	SAMSO, POB 92960, WWPC, LA, CA 9009
1	(DEE)
1	AFGL, Hanscom AFB, MA 01730
	AFATL, Eglin AFB, FL 32554
1	(DLOSL)
1	(DEE)
	RADC, Griffiss AFB, NY 13441
1	(Doc Lib)
1	(TUGF)
	AFRPL, Edwards AFB, CA 93523
1	(DYSN)
1	AFOSR, 1400 Wilson Blvd Arlington, VA 22209
	TAC, Eglin AFB, FL 32554
1	(DEE)
1	823 CES (HR), Eglin Aux Fld 9 FL 32544
1	CO, Diamond Lab (Lib), Wash, DC 20438
1	CO, USACDC, Inst Nuc Stud, Ft Bliss, TX 79916
	USAMC, RSIC, Redstone Arsenal, AL 35809
1	(Chief, Doc Sec)
1	(SENSC-DB)
	CO BRL, Aberdeen Pvg Gnd, MD 21005
1	(AMXBR-TB)
1	(AMXBR-BL)
1	(AMXBR-RL)

No. cys	
	CO, Picatinny Arsenal, Dover, NJ 07801
1	(SMUPA-TN)
1	CO, USARO, Box CM, Durham, NC 27705
1	Ch Eng (DAEN-RDM), Dept Army Rm 5G044, Forrestall Bldg Wash, DC 20315
	Dir, USA Eng WWES, POB 631, Vicksburg, MS 39181
1	(WESRL)
1	(WESSS) Joe Zelasko
1	Dir, NRL (2027), Wash DC 20390
1	Dir, NRL/EOTPO (5503) Wash, DC 20375
1	DO/Dir, NEL (4223), San Diego, CA 92152
1	Cdr. NWC (753), China Lake, CA 93555
1	OSC, Dept Navy, Wash DC 20360
1	CO, NWEF (ADS), Stop 40 Kirtland AFB, NM 87117
1	DDR&E (Asst Dir, Strat Wpns) Wash, DC 20301
	Dir, DIA, Wash, DC 20305
1	(DI-7D)
1	(DI-3)
1	Dir, OSD, ARPA (NMR) 1400 Wilson Blvd, Arlington, VA 22209
1	Cdr, FC DNA (FCPR), Stop 44 Kirtland AFB, NM 87115

DISTRIBUTION (cont'd)

No. cys	
1	Dir, WSEGp (Doc Cont) Wash, DC 20305
1	JSTPS (JLTW), Offutt AFB, NE 68113
1	ERDA (Lib), Rm J-004 Wash, DC 20545
1	LLL (Lib), Bldg 50, Rm 134 Berkeley, CA 94720
2	DDC (TCA), Cameron Sta Alexandria, VA 22314
1	GE TEMPO/T. Barret, 816 State Santa Barbara, CA 93102
	NRL, Wash, DC 20390
1	Code 2070
1	J. Boris
	NSWC, Wht Oak, Slvr Sp, MD 20910
1	Code 730
1	J. Peters
1	Exp Eff Div, Mr. Hornig
	DNA, Wash, DC 20305
2	DDST, Dr. Atkins, Mr P Haas
2	STTL
6	SPSS, E. Sevin; Capt J. Stockton; Maj T. Strong; K. Goering Dr. Ulrich
4	SPAS, J. Moulton; M. Rubenstein, Capt Garrison, Maj Anderson
1	STAP
3	RAAE, P. Fleming; Capt Mueller, Maj Bigoni
1	RATN, Cmdr Alderson
1	ODDR&E/Asst Dir, Strat Wpns, Wash D C 20301

No. cys	
1	ARPA/LtC Whitaker 1400 Wilson Blvd Arlington VA 22209
1	JSTPS/Maj Greene, Offutt AFB, NE 68113
1	DIA/Mr Castlebury Wash, DC 20305
	Sandia Lab, Kirtland AFB NM 87115
1	Org 3141
1	Div 1111
1	Org 1723, G.E. Barr
1	Div 5644, J. Reed
3	M. Merrit; L. Vortman; D. Dahlgren
	Sandia Lab POB 969 Livermore, CA 94550
1	Org 8000, Dr. Cook
1	R. Scholer
1	T. Gold
1	J. Mansfield
	LLL, POB 808 Livermore, CA 94550
1	L-51, M. Hanson
1	TID
1	Jeff Thompson
	LASL, POB 1663, Los Alamos NM 87544
1	Rpt Lib
2	J-10, E. Jones; R. Gentry
	Aerospace Corp POB 92957, LA, CA 90009
1	Lib
1	R.L. Beck
	Brn Eng Co, 300 Sparkman Huntsville, AL 35807
1	V. Kenner, MS-44
1	C. Wayne
1	J. Dobkins
	McDon Doug, 5301 Balso Huntington Beach, CA 92547
8	K.Stone; P. Lewis; D. Dean; T. Thomas; D. Hildebrand; J. Logan; R. Zach, H. Herdman

DISTRIBUTION (cont'd)

No. cys	
2	Kaman Sci, CO Spgs, CO 80907 D. Pirio; D. Sachs
1	Kaman Av/J. Reutenik, 83 2nd Ave Burlington, MA 01803
4	MartMar, POB 5837, Orlando, FL 32805 R. Heffner; C. Washburn; H. Suguichi; D. Cooke
2	MRC, 1 Presidio, Sta Barbara, CA 93101 R. Christian; D. Sowle
2	SAI, POB 2351, La Jolla, CA 92037 C. Busch; R. Lowen
1	SAI/D. Hove, 101 Cont Bldg Ste 310, El Segundo, CA 90245
1	SAI/R. Hillendahl, POB 10268 Palo Alto, CA 94303
1	SAI/M. Tobrinen, Ste 808 1901 N. Ft Myer, Arlington, VA 22209
1	SAI/R. Clemens, 122 LaVeta Dr NE Albuquerque NM 87108
1	BTL/W. Troutman, Whippany, NJ 07981
1	Calspan/R. Deliberis, POB 235 Buffalo, NY 14221
1	ISI/W. Dudziak, 123 W. Padre Sta Barbara, CA 93105
1	Lockheed, 3251 Hanover Palo Alto, CA 94304
2	MITRE, Box 208 Bedford, MA 01730 S. Morin; J. Brown
1	CRT/M. Rosenblatt, 19720 Ventura Ste H Woodland Hills, CA 91364
4	R&D Assoc, POB 3580, Sta Monica CA 90403 H. Brode; C. Knowles; J. Carpenter R. Lelevier
1	MARA/S. Kahalas, 385 Elliot, Newton Upper Falls, MA 02164

No. cys	
	TRW Sys Gp, 1 Sp Pk Redondo Beach, CA 90278
1	Lib
2	A. Kuhl
1	J. Peterson
1	AVCO/G. Grant, 201 Lowell Wilmington, MA 01887
1	IDA, 400 Arm-Nav Dr Arlington VA 22202
1	ASD/I&L, Wash, DC 20301
1	ARM For Stf Col/Lib, Norfolk, VA 23511
1	Ind Col Arm For, Ft McNair, Wash, DC 20315
1	Nat War Col/Lib, Ft McNair, Wash, DC 20315
1	USAMC/AMCRD-RP-B Wash, DC 20315
1	USAEC/AMSEL-RD Ft Monmouth, NJ 07703
	USNCEL, Pt Hueneme, CA 93041
1	Code L31
1	CEC Ofcr
1	MIT/Dr. Hansen, 77 MA Ave Cambridge, MA 02139
1	Princeton U/PPL, Dr Bleakney Princeton, NJ 08540
	Un MI, POB 618, Ann Arbor, MI 48104
1	Rsch Soc Ofc
1	IS&T, G. Frantti
1	St Louis Un/Dr. Kisslinger 221 N. Grand, St Louis, MO 63100
1	Boeing/R. Carlson, Seattle, WA 98124
1	GATC/MRD Div Lib, 7501 N Natchez Niles, IL 60648

DISTRIBUTION (cont'd)

No. cys	
1	H&N Sp Pro Div/S. Smith 849 S Bwdy, LA, CA 90014
1	URS, 1811 Trousdale Burlingame, CA 94010
1	SWRI/M. Whitfield, 8500 Culebra San Antonio, TX 78228
1	Un IL/Dr. Newmark, Tal Lab R207, Urbana, IL 61803
1	IITRI, 10 W. 35 Chicago, IL 60616
1	RAC/Lib, McLean, VA 22101
1	ADC (ADSWO), Kirtland AFB, NM 87117, Stop 70
1	SACLO, Kirtland AFB, NM 87117, Stop 68
1	TACLOS, Kirtland AFB, NM 87117, Stop 67
	AFWL, Kirtland AFB, NM 87117
1	HO/Dr. Minge
2	SUL
1	DE
1	DEV
1	DEX
1	DY
1	DYS
1	DYV
10	DYT
1	DYX
20	Capt M. Stucker/DYT
20	Capt M. Fry/DYT
1	SA
1	SAB
1	SAS
2	SAT/Mr. Sharp, Mr. Murphy
1	SAW
1	ESD (DEE), Hanscom AFB, MA 01730
1	Official Record Copy Capt Mark Fry/DYT